Chemical Science

ROYAL SOCIETY OF CHEMISTRY

REVIEW

View Article Online
View Journal | View Issue

Cite this: *Chem. Sci.*, 2023, **14**, 3091

Conductive hydrogels for tissue repair

Yongping Liang, [a] Lipeng Qiao,[a] Bowen Qiao[a] and Baolin Guo *[ab]

Conductive hydrogels (CHs) combine the biomimetic properties of hydrogels with the physiological and electrochemical properties of conductive materials, and have attracted extensive attention in the past few years. In addition, CHs have high conductivity and electrochemical redox properties and can be used to detect electrical signals generated in biological systems and conduct electrical stimulation to regulate the activities and functions of cells including cell migration, cell proliferation, and cell differentiation. These properties give CHs unique advantages in tissue repair. However, the current review of CHs is mostly focused on their applications as biosensors. Therefore, this article reviewed the new progress of CHs in tissue repair including nerve tissue regeneration, muscle tissue regeneration, skin tissue regeneration and bone tissue regeneration in the past five years. We first introduced the design and synthesis of different types of CHs such as carbon-based CHs, conductive polymer-based CHs, metal-based CHs, ionic CHs, and composite CHs, and the types and mechanisms of tissue repair promoted by CHs including anti-bacterial, antioxidant and anti-inflammatory properties, stimulus response and intelligent delivery, real-time monitoring, and promoted cell proliferation and tissue repair related pathway activation, which provides a useful reference for further preparation of bio-safer and more efficient CHs used in tissue regeneration.

Received 10th January 2023
Accepted 20th February 2023

DOI: 10.1039/d3sc00145h

rsc.li/chemical-science

1. Introduction

Every cell in the human body is surrounded by a membrane with ion channels, which can produce a transmembrane voltage. Therefore, all cells *in vivo*, not only excited nerve and muscle cells, can generate and receive steady-state bioelectrical signals, which can be used as a key factor to regulate and control the number (cell proliferation and apoptosis), location (migration and orientation) and type (cell differentiation) of each cell. For example, the transepithelial potential (TEP) of intact skin was 10–60 mV, which varies between different parts of the body and epidermis. When the skin is injured, the TEP of the injured site is disrupted, resulting in an endogenous electric field (EF), directed from the

[a]*State Key Laboratory for Mechanical Behavior of Materials, and Frontier Institute of Science and Technology, Xi'an Jiaotong University, Xi'an, 710049, China. E-mail: baoling@mail.xjtu.edu.cn; Fax: +86-29-83395131; Tel: +86-29-83395340*

[b]*Key Laboratory of Shaanxi Province for Craniofacial Precision Medicine Research, College of Stomatology, Xi'an Jiaotong University, Xi'an, 710049, China*

Yongping Liang was awarded a PhD in biomedical engineering from Xi'an Jiaotong University in 2021 under the supervision of Prof. Baolin Guo. His research focused on the development of multifunctional cryogels and conductive hydrogels based on inorganic nano-functional materials and biomedical polymers, and their application in soft tissue repair and rapid hemostasis. Currently, Yongping Liang is an assistant professor at the Frontier Institute of Science and Technology at Xi'an Jiaotong University.

Baolin Guo received his PhD degree from the Department of Fiber and Polymer Technology in 2011 at the Royal Institute of Technology (KTH) under the supervision of Professor Ann-Christine Albertsson. He is a professor at the Frontier Institute of Science and Technology (FIST), Xi'an Jiaotong University. His research focuses on biomedical polymers including degradable conductive polymers for tissue engineering application, multifunctional hydrogels for wound healing, rapid hemostasis materials, tissue regeneration, adhesives, human motion sensing devices and controlled drug delivery systems.

edge to the inside of the wound, which can stimulate host cell proliferation and migration, and ultimately promote tissue growth and re-epithelialisation.[1,2] Recent experiments have shown that this type of bioelectrical signal mechanism may play a more prominent role than previously thought. For example, Zhao and his colleagues found that an endogenous EF can control the electrotaxis of cell migration in wound healing by affecting key signaling pathways such as PI3K/Pten (phosphoinositide 3-kinases/phosphatase and tensin homolog), membrane growth factor receptors and integrins.[2,3] And by adding electrical stimulation to repaired tissue, subsequent studies have confirmed that electrical stimulation (ES) can enhance the proliferation of fibroblasts and promote wound healing through the activation of the TGFβ1-ERK-NF-κB signaling pathway.[4] In addition, an external EF can also promote angiogenesis by stimulating endothelial cells to produce the VEGF,[5] and activate Rho-ROCK and PI3K-Akt signaling pathways.[6,7] These new discoveries in cell and tissue electrophysiological behaviors have inspired us to develop a new generation of biomaterials that can activate specific genes and stimulate tissue regeneration at the molecular level.

Conductive hydrogels (CHs), which combine the advantageous properties of hydrogels with the physiological and electrochemical characteristics of conductive materials, have received considerable attention. Their three-dimensional porous structure, hydrophilicity and controllable chemical and physical properties resemble the extracellular matrix in tissues, making them favourable substrates for cell growth, migration and proliferation.[8,9] Moreover, the use of CHs not only expands the coverage of current to the entire wound,[10] but also overcomes the inconvenience in use and high-voltage risk of electrode-based electrical stimulation strategies.[11] On the other hand, unlike non-CHs, CHs with high conductivity and electrochemical redox characteristics are useable for the detection of electric signals generated in biological systems and deliver electrical stimulation to regulate the activities and functions of cells and tissues. Recently, several reports of electricity auto-generating hydrogel dressings combined with triboelectric nanogenerators have further enriched the CH family.[12–17] These aforementioned properties make CHs have unique advantages in tissue repair. However, the current review of CHs mainly focuses on their application in sensors, and their potential for tissue repair has only been developed in recent years. Therefore, it is necessary and timely to review the role of conductive materials in tissue repair, which will play a guiding role for a wide range of scientists interested in the application of conductive materials.

Therefore, this paper mainly focuses on the new progress of CHs in tissue repair in the past five years. First, the design and synthesis strategies of carbon-based CHs, conductive polymer-based CHs, metal-based CHs, and ionic CHs, were briefly introduced. Subsequently, the applications of CHs in nerve, muscle, skin, and bone repair were discussed, and several beneficial functions of conductive materials for tissue repair were further listed. Overall, this review will provide a useful reference for further preparation of safer and more efficient CHs for tissue repair (Fig. 1).

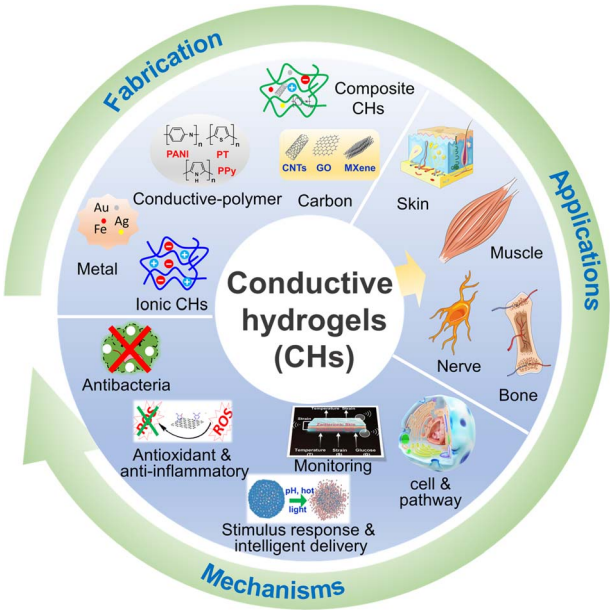

Fig. 1 Fabrication, applications and the mechanisms of CHs for tissue repair.

2. Fabrication of CHs for tissue repair

2.1 Carbon-based CHs

Benefitting from the good environmental stability, high conductivity and low production cost, carbon-based materials, including carbon nanotubes (CNTs), graphene, activated carbon, carbon fiber, carbon dots and porous carbon, are considered to be ideal materials for preparing CHs.[18,19] As a typical representative, carbon nanotubes and graphene-based conductive hydrogels have been widely explored.[20–24] Combined with the good *in situ* forming characteristics of hydrogels, a large number of CHs were prepared by simply mixing CNTs[25–34] or graphene oxide (GO)[20,35–38] into hydrogels and their application in promoting tissue repair was also verified. Among them, a cardiac-derived extracellular matrix protein,[26] π–π superposition provided by the pyrene group,[34] and Pluronic F127 (PF127)[29] were confirmed to promote the dispersion of CNT/GO in hydrogels. Although *in situ* physical encapsulation has the great advantage of a simple process, the potential hazards of conductive components after hydrogel degradation still cannot be ignored. Therefore, many modification tactics have been applied to improve the dispersion and immobilization of carbon-based materials in CHs, such as dopamine coating,[39–43] carboxyl functionalization,[30,44] amino modification,[45,46] double bond functionalization,[47] amphiphilic crosslinking agent-assisted,[48] PEG-modification[49] and β-cyclodextrin grafting.[50–52] For example, to further increase the dispersion of CNTs, carboxyl functionalized CNTs were selected and grafted to the end of PEG through esterification, which not only improved the surface hydrophilicity of CNTs but also reduced their aggregation.[49] And inspired by the dopamine chemistry, Liang and Zhao *et al.* prepared polydopamine coated CNT/graphene by dopamine/tannic acid self-polymerization under alkaline conditions, and prepared two kinds of multifunctional self-healing antibacterial antioxidant

conductive hydrogel dressings based on gelatin and hyaluronic acid (HA), respectively.[39,40,53] In the above example, the dispersion of CNTs/GO was greatly improved by polydopamine coated on the surface. At the same time, dopamine on the surface of CNTs/GO can also be used as a crosslinking agent to connect itself with dopamine grafted onto gelatin or hyaluronic acid by dopamine chemistry (Fig. 2A and B).[39,40] In addition, conductive biomedical hydrogels based on carbon nanofibers[54] and graphene quantum dots[55] have also been reported.

As the hottest two-dimensional nanomaterials, the booming transition metal carbide, nitride, or carbon nitride (MXene) family emerge due to its advantages of metal conductivity, high aspect ratio, solution processability and wide tunability.[56] When MXenes are incorporated into a hydrogel system, they provide an exciting multifunctional platform for the CHs used in tissue repair.[57–61] For

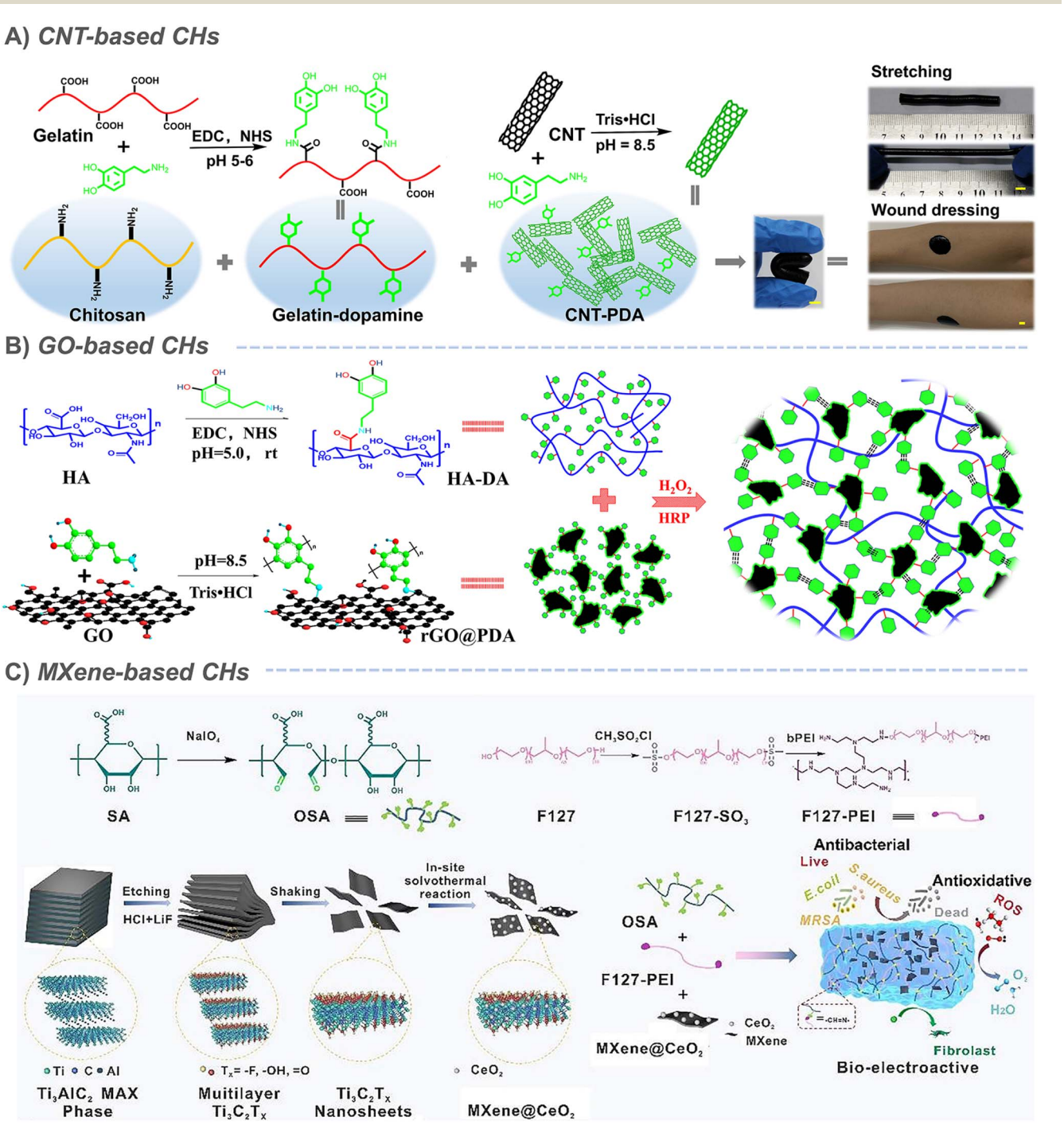

Fig. 2 Carbon-based CHs. (A) CNT-based CHs. Reproduced from ref. 39 with the permission of Elsevier, copyright 2019. (B) Graphene oxide (GO)-based CHs. Reproduced from ref. 40 with the permission of Wiley-VCH, copyright 2019. (C) MXene-based CHs. Reproduced from ref. 57 with the permission of Elsevier, copyright 2021.

example, when ultra-small CeO_2 nanoparticles were uniformly deposited on Ti_3C_2Tx MXene nanosheets by the facial hydrothermal method to form a MXenes@CeO_2 heterogeneous structure, they could endow CHs with antioxidant properties (Fig. 2C).[57] The polydopamine coating also gives MXenes better tissue adhesion.[58] With the assistance of light, MXenes were introduced as a microchemical reaction center to form hydrogen bonds and covalent bonds with ε-polylysine (ε-PL)/polyvinyl pyrrolidone (PVP), which accelerated the formation of an ε-PL/PVP hydrogel.[62] However, most of the reported MXene hydrogels are based on $Ti_3C_2T_x$, which is the most mature member of the MXene family in terms of synthesis and property research. Therefore, there is still much room for further optimization of MXene-based hydrogels for target applications. In general, CHs based on carbon-based materials have been widely developed, but are limited by their potential *in vivo* thrombosis and metabolic risks, and their use still needs to bwe carefully considered. But at the same time, it should also be noted that according to the different use scenarios, the defect will not necessarily seriously restrict its development. For example, in skin wound repair, the potential problems of carbon-based CHs can be almost ignored because they only come into contact with limited skin wounds.

2.2 Conductive-polymer-based CHs

Organic polymers are usually not conductive. It was not until Shirakawa, MacDiarmid and Heeger found the conductivity of a halogen-doped crystalline polyacetylene film in 1977 that organic conductive polymers began to enter people's vision. The conjugated π electrons generated in the polymer backbone can be effectively delocalized along the polymer chain, resulting in charge transfer along the polymer chain, thus exhibiting conductive behavior.[63–65] On this basis, conductive polymers such as polyacetylene (PA), polyaniline (PANI), polythiophene (PT) and polypyrrole (PPy) were successively developed. However, due to the aromatic ring on the skeleton, conductive polymers are essentially hydrophobic.[65,66] Therefore, the combination of conductive polymers and hydrogels to prepare CHs greatly expands the application of conductive polymers in biomedicine.[64,67] Our research group has long been committed to the preparation of conductive materials based on aniline oligomer/PANI and its application in the biomedical field. Based on the previous research on conductive polymers,[68–71] we introduced an aniline trimer and aniline tetramer into hydrogels, through the amide/ester bond constructed by the amino group on the aniline trimer, and the hydroxyl group on poly(-glycerol sebacate) (PGS),[72] PCL-PEG[73] or dextran[74,75] with the cyanic acid group on hexamethylene diisocyanate (HDI), the Schiff base bond between the amino group on the aniline trimer and the aldehyde group on oxidized hyaluronic acid,[76] the amide bond between the carboxyl group on the carboxylated aniline trimer and the amino group on chitosan.[77] In addition to chemical grafting, *in situ* polymerization is also an effective strategy for constructing CHs with uniformly dispersed conductive polymers. So, by *in situ* polymerization of aniline under the action of ammonium persulfate, Zhao *et al.* grafted PANI onto quaternized chitosan, and further crosslinked it by using oxidized-dextran[78] and benzaldehyde modified polyester[79] to construct PANI-based CHs for skin wound repair (Fig. 3A).[79] In some other study by Wu *et al.*, the crosslinking agent was replaced by benzaldehyde-terminated PEG[7] and *N*-acryloyl glycinamide.[80] However, its need for acid doping to exert conductivity seriously limits its further application.

Similarly, *in situ* polymerization of pyrrole was also used to prepare CHs with uniformly dispersed PPy. In an example, during the crosslinking process of APS-triggered double-bonded chitosan, PPy was *in situ* polymerized to form chitosan-modified PPy nanoparticles, which were further loaded into a Schiff base hydrogel through electrostatic interaction.[81] In addition, further studies also confirmed that chitosan contributed to the dispersion of the pyrrole monomer and enhanced the uniformity of PPy in PPy-chitosan hydrogels formed by *in situ* polymerization.[82,83] Liu *et al.* achieved a complete end-capping through the reaction of the pyrrole monomer with the acrylate group at the end of the hyperbranched polymer. Subsequently, Fe^{3+} was used to *in situ* polymerize pyrrole[84] to form conductive PPy nanoparticles, which can further act as crosslinking sites to enhance the strength of the network and give the hydrogel conductivity (Fig. 3B).[85] However, the *in situ* polymerization method does not guarantee the complete reaction of the pyrrole monomer and may produce potential toxicity. Furthermore, when PPy was directly mixed into a hydrogel,[86–88] its conductivity decreased due to the loss of the dopant in a weak alkaline physiological environment (pH 7.4), and is likely to leach, resulting in biological toxicity. In response to this problem, it has been shown that the covalent bond between 3-sulfopropyl methacrylate (3SPMA) and hydrogel could also prevent PPy leaching when an anionic 3SPMA monomer was copolymerized in the hydrogel to *in situ* doped PPy.[11] In some other typical examples, polydopamine is coated on the surface of PPy nanoparticles, which improves their dispersion in hydrogels;[89] meanwhile, the photothermal conversion ability of PPy can also realize NIR-assisted photothermal sterilization and reduce infection (Fig. 3B).[15,89] However, although this can effectively reduce the potential toxicity of PPy, it still cannot completely eliminate the hidden dangers.

Polythiophene has always been a topic of interest to many researchers. In a recent study, researchers combined the strong light absorption and conductivity of polythiophene with the efficient reactive oxygen species (ROS) generation characteristics of selenium viologens (SeV^{2+}), and then dipped it into a polyacrylamide hydrogel to prepare a new anti-sandwich photoelectronic wound dressing, which greatly improved the repair of infected wounds (Fig. 7A).[90] However, polythiophene is generally difficult to disperse in water. So, as one of the most widely used polythiophenes, hydrophobic poly(3,4-ethylenedioxythiophene) (PEDOT) is surrounded by a hydrophilic poly (styrene sulfonate) (PSS) shell to form PEDOT:PSS nanoparticles, which can be easily suspended in water buffer. In a typical example, PEDOT:PSS was used for bioprinting with gelatin methacryloyl (GelMA) to form a complex 3D cell load structure. In addition to the photopolymerization of GelMA under visible light, PEDOT:PSS can also form secondary crosslinking with Ca^{2+} to enhance the network (Fig. 3C).[91] It has also been found that both boron nitrogen

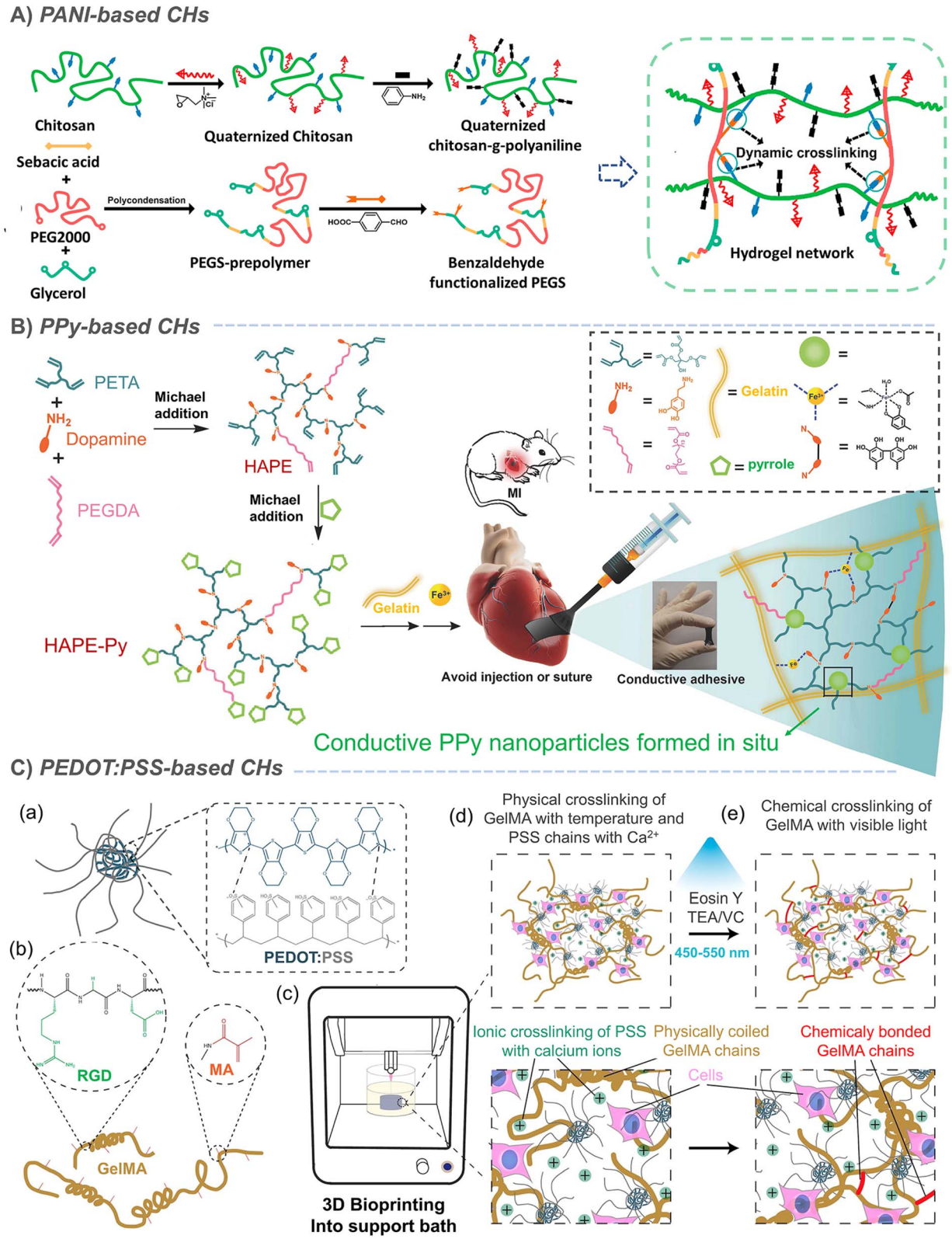

Fig. 3 Conductive-polymer-based CHs. (A) PANI-based CHs. Reproduced from ref. 79 with the permission of Elsevier, copyright 2017. (B) PPy-based CHs. Reproduced from ref. 85 with the permission of Wiley-VCH, copyright 2018. (C) PEDOT:PSS-based CHs. Reproduced from ref. 91 with the permission of American Chemical Society, copyright 2019.

nanosheets and poly(*N*-isopropylacrylamide) (PNIPAM) can form sufficient dynamic hydrogen bond crosslinking points with PSS, which not only ensured the self-healing and adhesion of PNIPAM-based hydrogels, but also enhanced the conductivity of PEDOT:PSS due to the weakened Coulomb interaction between PEDOT and PSS chains.[92] In the above example, PSS acts as a dopant to increase the dispersion of PEDOT in water. Similarly, sulfated alginate[93] and chitosan[94] have also been proved to achieve similar effects, but this should not be as effective as PSS. In conclusion, CHs based on conductive polymers have been greatly developed, but uneven dispersion, monomer toxicity and other issues are still the main factors that plagued their development.

2.3 Metal-based CHs

Metals have high conductivity, interesting optical and catalytic properties, and are easy to manufacture and modify. Therefore, CHs based on metal nanomaterials have also been studied in the field of tissue repair recently. Among all the common metals, Ag is the most widely used one in biological materials. In addition to conductivity, Ag also has strong antibacterial properties, and it also has been approved by the FDA. So, a large number of Ag-based biomaterials are used for antibacterials in burn and infection wound treatment.[95] In the presence of a reducing agent, it is easy for silver ions to form Ag nanoparticles *in situ* and easy for them to be loaded into hydrogels, which further expand their application. For example, in the presence of sodium borohydride ($NaBH_4$), a rapid formation of silver nanocomposite CHs was achieved *via in situ* addition of guar gum-grafted-polyacrylamidoglycolic acid polymer, and silver nitrate ($AgNO_3$) (Fig. 4A).[96] Another study also confirmed that silver ions can catalyze radical polymerization by converting water molecules into hydroxyl radicals in the presence of ammonium persulfate, and further *in situ* formed hydrogels.[97] An interesting phenomenon is that, lignin with antioxidant properties can *in situ* reduce silver to form an Ag-lignin nanoparticles,[98] which can trigger a dynamic oxidation–reduction environment, continuously produce catechol groups, and endow CHs with long-term and repeatable adhesion.[99] And the self-polymerization of the dopamine structure can also form a coating on the outer layer of silver nanoparticles.[100] In addition to nanoparticles, silver nanowires are also used as crosslinking units to prepare CHs.[101] For example, when silver nanowires were combined with methacrylic acid alginate, they can be printed on medical-grade patches for personalized wound treatment.[102] However, in addition to the toxicity of silver itself and the potential thrombosis risk of nanoparticles, the *in situ* formation characteristics that bring the advantages of silver nanoparticles will also be accompanied by the introduction of toxic reducing agents during their preparation. All these make the application of silver full of indeterminacy.

In addition to silver, gold is also a metal that was often used in conductive biological materials, and gold nanoparticles[103] and nanorods[104] have been used to construct CHs. For example, when gold nanoparticles were encapsulated into semiconductor-like metal organic framework ZIF-8, and then loaded into an injectable Schiff base hydrogel, the photocatalytic ROS generation properties of gold nanoparticles in this hydrogel under visible light played an antibacterial role and further promoted tissue repair.[105] Besides, injectable CHs containing gold, LAPONITE® nanoparticles, and an extracellular matrix of cardiomyocytes can improve phenotypic maturation of heart-specific protein.[106] Like Ag, the potential nanotoxicity is also a bottleneck that restricts the development of gold nanomaterials.

In addition, the introduction of Fe^{3+} was considered to significantly improve the conductivity of hydrogels, and the coordination between Fe^{3+} and carboxylic acids and catechol also enhanced the strength of hydrogels with poly(thioctic acid) as the skeleton structure and composited with polydopamine (PDA).[107] Besides, a gallium-based liquid metal alloy circuit was also encapsulated into an adhesive based on polyethylene glycol (PEG) mixed polydimethylsiloxane (PDMS) to form an epidermal electronic device.[108] And CHs based on dopamine crosslinking between polydopamine coated GeP nanosheets and dopamine modified hyaluronic acid have also been developed.[109] In general, metal-based CHs have been widely developed, but also limited by the potential toxicity of nanomaterials, so further efforts are still needed.

2.4 Ionic CHs

Some studies suggest that when electronic conductors (such PPy, CNT, PANi and rGO) are incorporated into hydrogels to provide conductivity, they always transmit discontinuous electrical signals as information carriers, while the biological system essentially transmits continuous signals through ions. In addition, electronic conductors often have many problems, such as uneven dispersion and conductive paths, unresolved toxicity and so on. In contrast, ion-based CHs have become a global hot topic because they have the required flexibility, good conductivity and adjustable mechanical properties.[110] At the same time, the hydrogel is macroscopically similar to a solid, but microscopically exhibits liquid properties. Such characteristics also provide rich channels for ion migration. This feature contributes to the charge conversion between ionic CHs and tissues, and provides a possibility for their application in tissue repair.[111] Based on the interaction between positive and negative charges, a large number of ionic crosslinked CHs have been constructed. A typical representative should be hydrogels formed by ion-metal coordination between metal ions and a carboxyl-containing polymer, which include polysaccharides like hyaluronic acid and alginate, and synthetic polymers like polyacrylic acid. For example, tri-crosslinked conductive self-healing hydrogels containing sodium alginate, acrylamide, acrylated dopamine, acrylated guanine and Ca^{2+} were constructed by using UV irradiation.[112] And macroporous ionic CHs were formed by introducing biocompatible polyacrylic acid (PAA) into an oxidized alginate (OSA)/gelatin (GT) hydrogel matrix. By changing the concentration of PAA, the ionic conductivity (up to $35.36 \pm 7.72 \times 10^{-3}$ S cm^{-1}) and mechanical properties (up to 37.04 ± 2.75 kPa) of this hydrogel can be easily adjusted to match the requirements of cardiac tissue (Fig. 4B).[110] Besides, in the classical conductive polymer PEDOT:PSS, anionic PSS chains can not only increase the dispersion of PEDOT, but also interact with positively charged molecules. For example, when cationic guar gum is combined with PEDOT:PSS, conductive injectable self-healing hydrogel dressing can be rapidly prepared in one minute

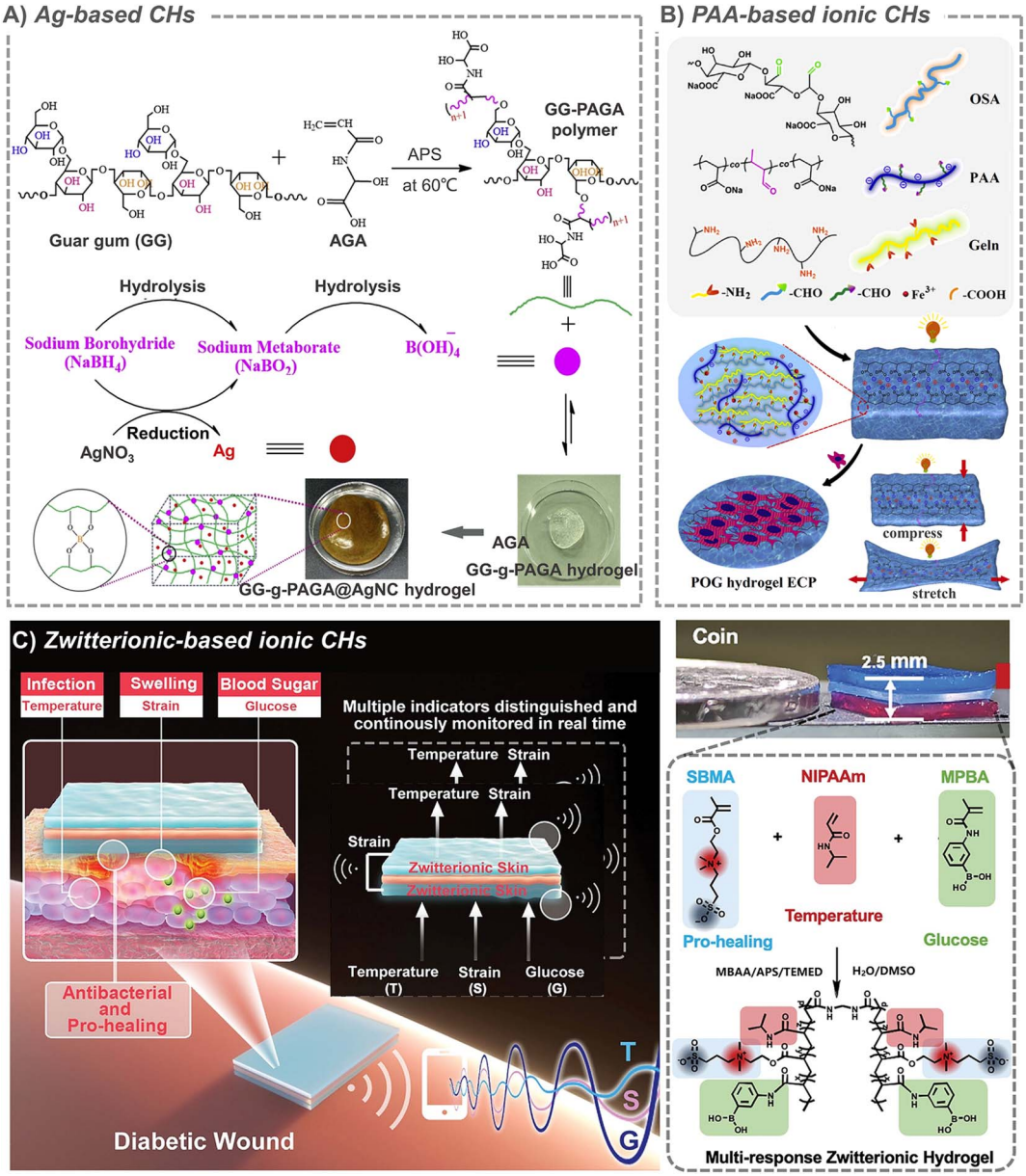

Fig. 4 Metal-based and ionic CHs. (A) Ag-based CHs. Reproduced from ref. 96 with the permission of Elsevier, copyright 2019. (B) PAA-based ionic CHs. Reproduced from ref. 110 with the permission of Elsevier, copyright 2021. (C) Zwitterion-based CHs. Reproduced from ref. 114 with the permission of Wiley-VCH, copyright 2021.

for wound healing in various sports.[113] However, the stability of these CHs cannot be guaranteed when the anions and cations begin to move freely due to conduction.

Another kind of ionic conductivity is derived from amphoteric ions. Because of their unique structure with the same positive and negative charges, amphoteric ions are known for their excellent biocompatibility and high hydrophilicity. In a typical example, based on zwitterionic carboxyl betaine, temperature-responsive *N*-isopropylacrylamide and glucose-responsive methylacrylamide phenylboric acid, multi-responsive skin-like ionic CHs were developed and they could even produce/detect electrical signals in response to the temperature, strain, and glucose concentration (Fig. 4C).[114] Another zwitterion poly[3-(dimethyl(4-vinylbenzyl) ammonium) propyl sulfonate] (SVBA) was also introduced into a poly-acrylamide network, to prepare a conductive dressing with effective antibacterial properties, strong adsorption, high permeability and good electrical activity.[115]

However, ionic conductivity depends on the free movement of anions and cations, and most of the ions in ionic CHs are limited to varying degrees within the hydrogel, which greatly limits the application of ionic CHs. So, when sodium chloride is introduced into a chitosan-based hydrogel, the migration of chloride ions and sodium ions in the hydrogel matrix makes them have excellent conductivity.[116] And the ionic conductivity was also achieved by incorporating lithium chloride salt into organic hydrogels.[14] Besides, the introduction of ionic liquids also brings new members

to ionic CHs. In one case, the imidazolidine ionic liquid monomer and acrylamide were first polymerized by using free radicals, and then mixed with 10% PVA solution for 5 freeze–thaw cycles to form a polyvinyl alcohol/acrylamide-ionic liquid hydrogel. The introduction of ionic liquid not only endows the hydrogel with broad-spectrum antibacterial activity against bacteria and fungi, but also endows it with excellent conductivity (1.04 S m^{-1}).[117] Similarly, another polymeric ionic liquid 1-vinyl-3-(3-aminopropyl)-imidazolium tetrafluoroborate ($VAPimBF_4$) was also used to develop multifunctional CH dressings with konjac glucomannan.[10] However, toxicity and ion leakage are still the biggest obstacles restricting the application of ionic liquids. But this does not hinder the rapid development of ionic liquids in tissue sensing, and some recent reviews have also been well organized in this regard.[118,119]

2.5 Composite CHs

In addition to the above CHs, some composite CHs have also been developed, such as a hydrogel/fiber composite scaffold with conductivity in both hydrogel and fiber phases, which is fabricated by electrospinning of PANI-based fibers, and then followed by mixing with the hydrogel precursor solution that is composed of oxidized polysaccharides, gelatin and graphene.[120] Similarly, some CHs combining carbon-based materials and conductive polymers, such as CNTs and PPy,[121] and CNTs and PEDOT:PSS,[122] were also developed. In addition, conductive boron nitride nanosheets (f-BNNS) are also used to bind to PEDOT:PSS, and the dynamic hydrogen bond crosslinking point formed between PSS and f-BNNS also greatly improved the mechanical properties of the composite CHs.[92] On the other hand, PANI is also used to combine with polydopamine modified silver nanoparticles and PVA to construct CHs by supramolecular assembly. Due to the conductivity provided by Ag NPs and PANI, the hydrogel was used for real-time monitoring of large-scale human movement and showed a good therapeutic effect in diabetic skin wounds.[100] And a composite nano-CH based on silver-nanoparticles-decorated reduced GO nanosheets was also prepared by *in situ* reduction of GO by using silver.[123] In addition, graphene is also combined with zinc oxide[124] and CNTs[125] to prepare CHs. However, most of the mixing of conductive components lacks a certain chemical reaction at present, and is limited to simple mixing. Moreover, the conductivity of composite CHs has not been greatly improved in order of magnitude, and the conductivity of hydrogels based on atomic conductivity still lags far behind that of ionic CHs. When the two are combined, atomic conductivity can almost be ignored.

3. CHs for various tissue repair applications

3.1 Nerve tissue repair

Considering the inherent existence of an EF and synapses in the nervous system, conductive biomaterials are widely used to enhance nerve regeneration. CHs improve cell behaviors through physical morphology, and chemical and biological activities, and provide appropriate nutrition for nerve tissue regeneration.[126] So, in this section, we will summarize the recent advances in CHs to enable neural regeneration.

Studies have shown that the neurite development on the composite CH based double bond functionalized GO/CNT is strongly stimulated,[47] and the growth of neurites in the hydrogel loaded with 20 μg mL^{-1} SWCNT increased by 3.3 times (Fig. 5A).[30] The nerve regeneration ability of CHs containing *in situ* formed PPy nanoparticles was also confirmed by the recovery of motor function in a zebrafish brain injury model.[81] In further study of rats with spinal cord injury, collagen/hyaluronic acid hydrogels loaded with bone marrow mesenchymal stem cells (BMSCs) and conductive antioxidant bifunctional polypyrrole nanoparticles protect BMSCs from oxidative damage, restore bioelectrical signal transmission, inhibit secondary damage, and promote neuronal differentiation through a synergy between conductivity and electrical stimulation, resulting in significant nerve regeneration and functional recovery (Fig. 5B).[88] In another example, a CH using tannic acid as the crosslinking agent and dopant was prepared by using electrostatic interaction between the protonated nitrogen group on PPy and the phenolic hydroxyl group on tannic acid. This strategy effectively simulates the 3D soft mechanical properties and electrical transport functions of natural spinal cords.[127] However, the stability of crosslinking based on electrostatic interaction is still doubtful.

The recruitment of endogenous stem cells and wound regeneration are two important aspects of promoting *in situ* nerve regeneration. However, current strategies rarely combine both. So, through 3D coaxial printing, researchers constructed a self-adaptive integrated delivery chip with a chemokine-anchored outer CH shell and an enzyme-initiated vector/plasmid DNA composite inner microchannel, which realized therapeutic protein release, gene delivery and electrical conduction, and significantly enhanced endogenous mesenchymal stem cell recruitment during nerve tissue repair.[128] A PPy-based microfluidic hollow hydrogel fiber, which combines sodium alginate and polyacrylamide, has a conductivity of 0.32 S m^{-1} which is higher than that of the natural sciatic nerve. It was further found that the release of an endogenous nerve growth factor (NGF) in Schwann cells could also be driven by the use of a figure-eight coil to generate electromotive force through electromagnetic induction, which contributed to the synergistic effect of bioelectricity and neurotrophic factors on nerve repair.[129] In another example, researchers have obtained a granular hydrogel with jamming-induced elasticity, repeatable injectability, shear-thinning and self-healing, and high conductivity (about 10 S m^{-1}) by breaking the PEDOT:PSS-based bulk hydrogel. This granular microstructure enables them to easily encapsulate neural progenitor cells derived from an induced pluripotent stem cell (iPSC).[130] However, the conductive materials mentioned in the above studies lack an effective spatial structure. Inspired by the physiological structure of the peripheral nerve, with the help of the hierarchical nanostructures of a *Morpho* butterfly wing, researchers first performed oxygen plasma treatment on the wings to obtain hydrophilic surfaces, and then further introduced hydrohalic acid reduced GO nanosheets. Finally, a brain-derived neurotrophic factor (BDNF) was compounded and GelMA was used to achieve gelation and encapsulation of the above substances.

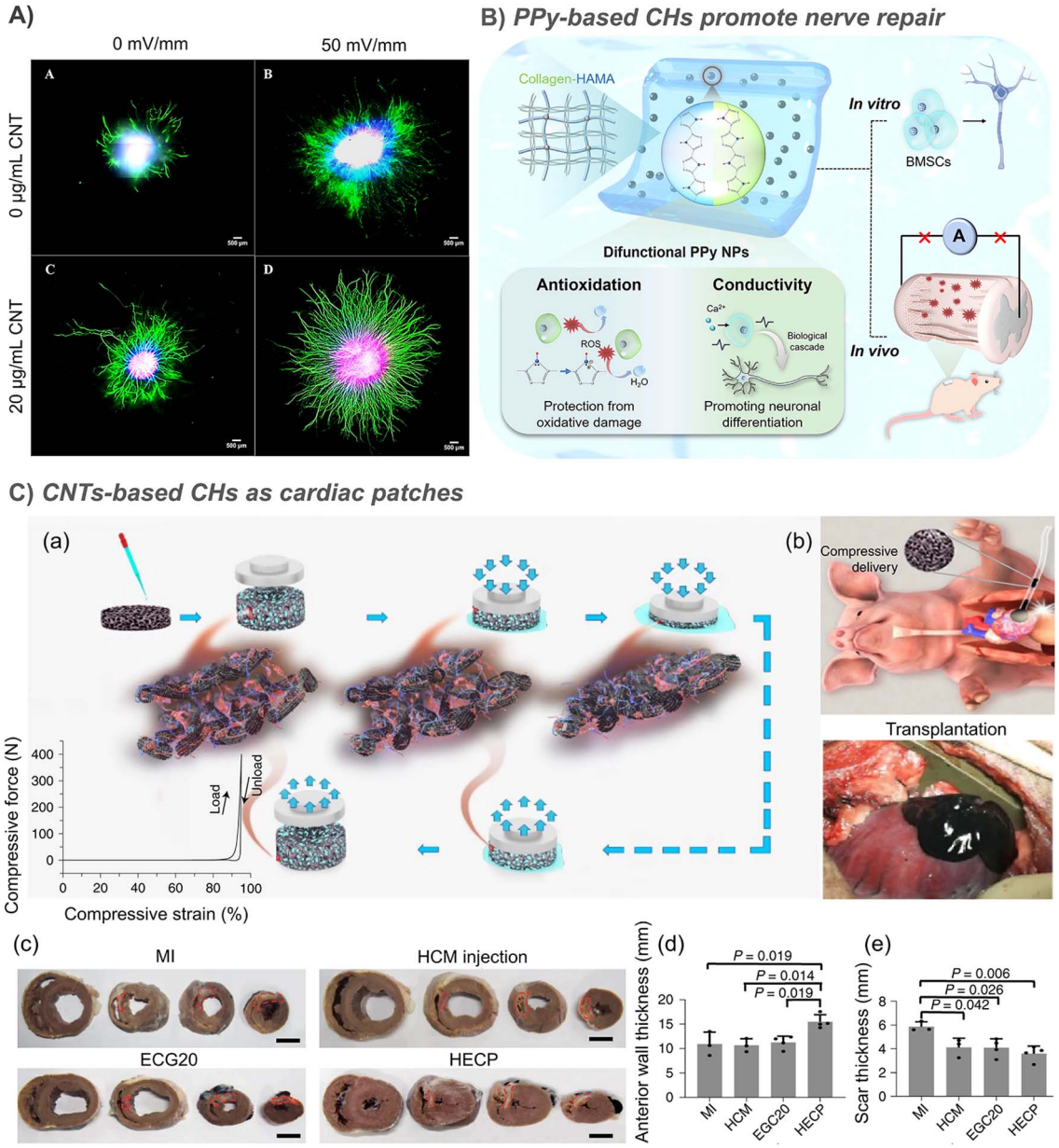

Fig. 5 CHs for nerve and muscle repair. (A) The growth of neurites in the hydrogel loaded with 20 μg mL^{-1} SWCNTs increased by 3.3 times. Reproduced from ref. 30 with the permission of Elsevier, copyright 2016. (B) Collagen/hyaluronic acid hydrogels loaded with bone marrow mesenchymal stem cells (BMSCs) and conductive antioxidant bifunctional PPy nanoparticles protect BMSCs from oxidative damage, and promote nerve regeneration and functional recovery through a synergy between conductivity and electrical stimulation. Reproduced from ref. 88 with the permission of American Chemical Society, copyright 2021. (C) CNT-based injectable and conductive cardiac patches. (a) The methacrylated elastin-gelatin cryogel cardiac patches loaded with CNTs was prepared by low temperature crosslinking of double bonds. And the patches support a compression force of about 400 N at 95% strain. (b) The injection diagram of the patches and the patches injected into the lesion site. (c) After 4 weeks of treatment, the representative multi-layer cross-section of the pig heart in the myocardial infarction (MI) control group, human cardiomyocyte (HCM) injection treatment, EGC20 patch implant treatment, and the HCM-EGC20 cardiac patch (HECP) treatment group. Statistical data of the (d) anterior wall thickness and (e) scar thickness of the left ventricle in different treatment groups. Reproduced from ref. 33 with the permission of Springer Nature, copyright 2021.

Finally, the hydrogel scaffold not only showed the ability to promote an increase in the neural stem cell neurite length and guide cell orientation, but also showed good performance in repairing 10 mm sciatic nerve defect in rats.[30,47,131] However, the biosafety of this bio-based material and the differences between different batches are still issues that cannot be ignored. And due to the physical nature of the hydrogel material, it is still difficult to induce nerve growth in a directed manner like nerve conduits, and it is also difficult to achieve nerve growth and docking inside the hydrogel.

3.2 Muscle tissue repair

The contraction activity of muscle tissue is responsive to electrical signals. Therefore, CHs with similar conductivity to that of natural muscles are promising candidates for muscle tissue engineering scaffolds. Based on our previous study on the enhancement of intercellular interaction, maturation and the synchronous calcium transient of neonatal rat primary myocardial cells (CMs) by using aniline trimer based electroactive elastomers with micropatterned surfaces,[72] we further prepared 3D aligned conductive cryogels with conductive and anisotropic compression properties based on polydopamine coated CNTs by the one-way freezing technique, and proved that it was a promising scaffold candidate for skeletal muscle tissue engineering.[132] Cell therapy is a promising strategy for regenerating heart tissue for myocardial infarction. Therefore, based on the dynamic Schiff base crosslinking between a chitosan-aniline tetramer (CS-AT) and dibenzaldehyde-terminated polyethylene glycol (PEG-DA), our group prepared injectable self-healing CHs as cell delivery carriers for myocardial infarction. The conductivity of the hydrogel is about 10^{-3} S cm^{-1}, which is very close to that of the natural heart tissue. C2C12 myoblast and H9C2 cardiomyocyte encapsulated hydrogels also showed good activity and release behavior.[77] Unfortunately, the study lacks further *in vivo* tests. Therefore, in a more complete study, melamine with a π–π conjugated ring was used to synthesize a multi-arm cross-linking agent PEGDA700-melamine, which further cross-links thiol modified hyaluronic acid (HA-SH) to construct injectable CHs after adding GO and adipose tissue-derived stromal cells (ADSCs). Subsequently, a rat myocardial infarction model was further used, and it was confirmed that these CHs significantly improve cardiac function, increase the ejection fraction (EF), and reduce the infarct size by increasing the expression of α-smooth muscle actin (α-SMA) and connexin 43 (Cx43).[35] However, this method of introducing conductive components through π–π interaction is not very strong. When applied to tissues such as the heart, it will cause great risks due to the leakage of nanomaterials at any time. In another study, based on the Fe^{3+} triggered simultaneous polymerization of pyrrole and bioadhesive dopamine on hyperbranched polymer chains, a paintable hydrogel with conductivity ($6.51 \pm 0.12 \times 10^{-4}$ S cm^{-1}) comparable to the normal myocardium ($\approx 10^{-4}$ S cm^{-1}) can be tightly adhered to the beating heart within four weeks, thus effectively promoting the transmission of electrophysiological signals. Finally, cardiac function reconstruction and myocardial infarction revascularization were significantly improved (Fig. 3B).[85,133] Besides, by grafting an aniline tetramer and 4-formylbenzoic acid onto dextran and further combining it with *N*-carboxyethyl chitosan (CEC), our group constructed an injectable self-healing CH based on a Schiff base, which showed sufficient electrical activity and a conductivity of about 10^{-2} mS cm^{-1}. Based on the self-healing ability, this hydrogel can encapsulate cells *in situ* and support the continuous release of C2C12 myoblasts, which promotes the regeneration of skeletal muscle in a volumetric muscle loss injury model.[75] Recently, we further developed a conductive porous nanocomposite cryogel based on gelatin (GT) and reduced graphene oxide (rGO), and further loaded muscle-derived stem cells to significantly improve the production of new muscle fibers and blood vessels.[134] In addition, studies have shown that PAA can endow hydrogels with micro-uniform conductivity. Compared with the cardiomyocytes in a hydrogel embedded with an electronic conductor, the cardiomyocytes cultured in the PAA composited hydrogel showed better orientation and elongated sarcomeres. After the hydrogel containing PAA was implanted in rats with myocardial infarction, it significantly inhibited cardiac fibrosis, promoted cardiac recovery and new capillary formation (Fig. 4B).[110] As a conductive nanomaterial, CNTs have been confirmed to support the growth of cardiomyocytes and stimulate action potential in cardiomyocytes, and to simulate the role of the Purkinje network.[135] In order to obtain high conductivity, an ultra-high CNT concentration (20 mg mL^{-1}) was incorporated into an injectable macroporous cryogel based on methacryloyl gelatin and methacryloyl elastin. Subsequent studies have shown that the scaffold can promote myocardial cell maturation, calcium transient and synchronous contraction, and improve the electrical response and left ventricle pumping function of the infarcted heart in rats with myocardial infarction.[33] However, the anatomical structure and beating characteristics of a rat heart are different from those of a human heart, which also affects the reliability of the experimental results. Therefore, the researchers further tested the effect of a scaffold loaded with cardiomyocytes differentiated from human pluripotent stem cells on cardiac function recovery in porcine myocardial infarction (Fig. 5C).[33] But the ultra-high concentrations of CNTs may cause potential thrombosis risk, which is still a huge hidden danger that cannot be ignored.

3.3 Skin tissue repair

The conductivity of normal skin tissue ranges from 10^{-7} to 2.6×10^{-3} S cm^{-1}.[136] Studies have confirmed that after a skin defect is generated, the positive charge in the wound combines with the negative charge around the entire skin to form an endogenous EF,[2] which is conducive to the migration of macrophages, neutrophils and keratinocytes in the closure of the wound. However, wound defects are often not conducive to the smooth charge transfer of the endogenous EF. Therefore, additional EF stimulation has been introduced as an alternative method (Fig. 6),[137,138] because it has been shown to guide the migration and proliferation of epithelial cells and fibroblasts by activating ion channels and downstream transduction signals, as well as inducing angiogenesis and immune regulation.[102] However, an external electrical stimulation device also has the disadvantages of large volume, low wound adaptability, easiness to cause skin inflammation and mental stress. Moreover, due to the larger impedance of human skin (∼MΩ cm^{-2}) clinically used direct current stimulation may require a higher voltage, which is harmful to the human body. Fortunately, the use of CHs to cover the wound can effectively assist electrical stimulation therapy, conducting current to the entire wound area.[11,139] This has attracted wide attention in the past few years, and related research has shown a rapid growth trend.[66,67,73–75,140–142]

Based on our previous research on conductive polymers, Zhao *et al.* applied PANI-based CHs to skin wounds in 2017, and confirmed that CHs containing PANI could better promote skin tissue repair (Fig. 3A).[79] Since then, various CHs have been developed to deal with different types of skin wounds. For an incisional

wound, the coordination of protocatechuic aldehyde and Fe^{3+} enhanced the tissue adhesion of the CHs.[143] For full-thickness wounds, tissue adhesion based on dopamine,[38,40,43,107] tannic acid,[32] *etc.* not only supports the durable and strong adhesion of CH dressings to the wound, but also gives the dressing antioxidant properties.[40,41,43] For example, in a CH based on the Schiff base reaction between *N*-carboxyethyl chitosan and an oxidized HA-aniline tetramer, the aniline tetramer not only exerts conductive properties, but also has antioxidant functions, which can effectively remove excess ROS generated at the wound site.[76] In addition, in the face of the first major problem that seriously threatens wound repair-bacterial infection, a large number of antibacterial CH dressings based on Ag,[97,99] antimicrobial peptides,[28] small molecule compound diphlorethohydroxycarmalol,[144] and drug silver sulfadiazine[24] have been developed to effectively control bacterial colonization. Adaptive CHs based on dynamic bonds adapt and fill the wound by changing their shape under the action of gravity or external force, and reconstruct their cross-linking network through the continuous cracking and regeneration of dynamic cross-linking bonds to promote the hemostatic repair of irregular or deep, complex and frequently moving wounds.[62,113,145] Furthermore, intelligent wound care strategies, including immediate monitoring and response to wound conditions and multi-tactile sensing reconstruction, have also been reported.[16] However, skin wound repair is a complex and continuous process, and conductive wound dressings that can truly coordinate and promote healing at various stages still pose great challenges.

The priority for infected wounds is bacterial control. Therefore, the antibacterial properties derived from antibiotic release,[20,23,29,39,40,73,76,142] photothermal properties of CNT,[29,39] GO,[20,23] and PPy,[146] and even the synergistic antibacterial of GO's photothermal antibacterial properties and BNN6's NO production antibacterial properties *etc.* have been reported to effectively control the bacterial reproduction in skin wounds, and promote healing.[51] In addition, the conductive PANI fragment had strong antibacterial activity against biofilms of *Pseudomonas aeruginosa* and *Staphylococcus aureus*, and also showed great application prospects in infected chronic wounds.[80,147] Under the dual stimulation of visible light and electricity, selenoviologen-appendant polythiophene (SeV^{2+}-PT)-containing polyacrylamide hydrogels can rapidly generate renewable and stable ROS, and quickly and efficiently kill bacteria (6 s), which shortens the healing time of full-thickness wounds infected by bacteria to 7 days (Fig. 7A).[90] Furthermore, for chronic wounds infected by typical drug-resistant bacteria MRSA, the dynamic redox system of Ag-lignin in CHs ensures lasting antibacterial properties and adhesion;[98] MXene@CeO_2 nanocomposites not only showed the photothermal antibacterial properties of MXenes, but also combines the antioxidant properties of CeO_2 (Fig. 2C);[57] Silver nanoparticle modified reduced GO nanosheets (Ag@rGO) synergize the dual antibacterial properties of Ag and photothermal properties of Ag@rGO;[123] and a triple antibacterial CH system combining antibiotic doxycycline sustained release, quaternary ammonium cations and photothermal properties of GO was also established (Fig. 9A).[20] Although photothermal antibacterial can kill bacteria efficiently and quickly, it should also be noted that short-term high temperature can also cause damage to surrounding tissues, which in turn inhibits repair. Therefore, appropriate temperature control in *in vivo* treatment to balance sterilization and tissue damage is still a problem.

In diabetic wounds, high glucose inhibits the production of hypoxia-inducible factor-lα (HIF-1α), which is the transcription factor that regulates the expression of the vascular endothelial growth factor (VEGF). So, researchers prepared a hydrogel that combines a hypoxia-inducible system with a conductive network by an original sequential interpenetrating technology

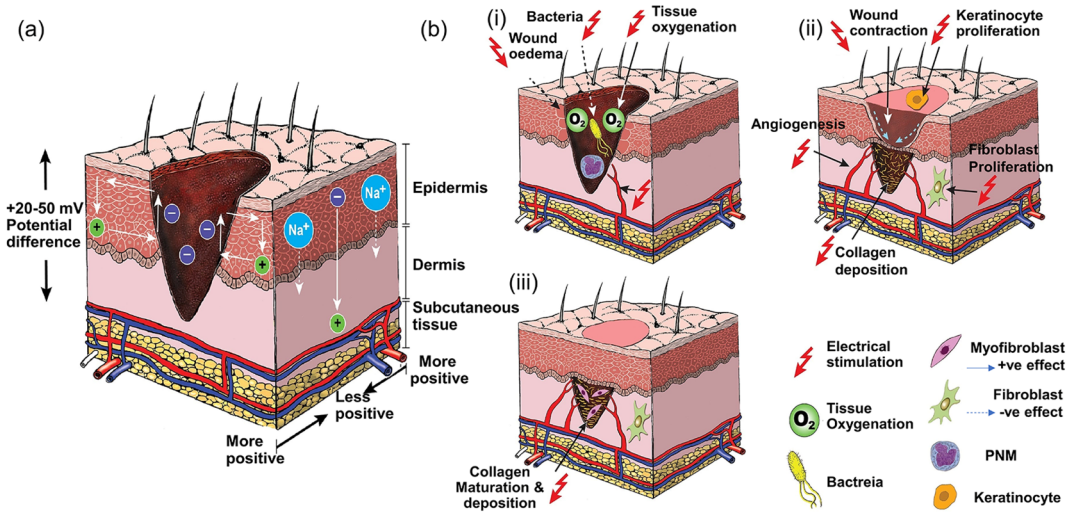

Fig. 6 Current of injury and effect of electrical stimulation on wound healing. (a) Normal skin has a transcutaneous current potential of 20–50 mV; injured skin generates injury current. (b) (i) Electrical stimulation enhances blood flow and tissue oxygenation, inhibits bacterial growth and decreases wound oedema in the inflammatory phase, (ii) increases wound contraction, keratinocyte and fibroblast proliferation, angiogenesis and collagen deposition in the proliferative phase, and (iii) enhances collagen maturation and remodeling in the remodeling phase of wound healing. Reproduced from ref. 138 with the permission of Wiley-VCH, copyright 2017.

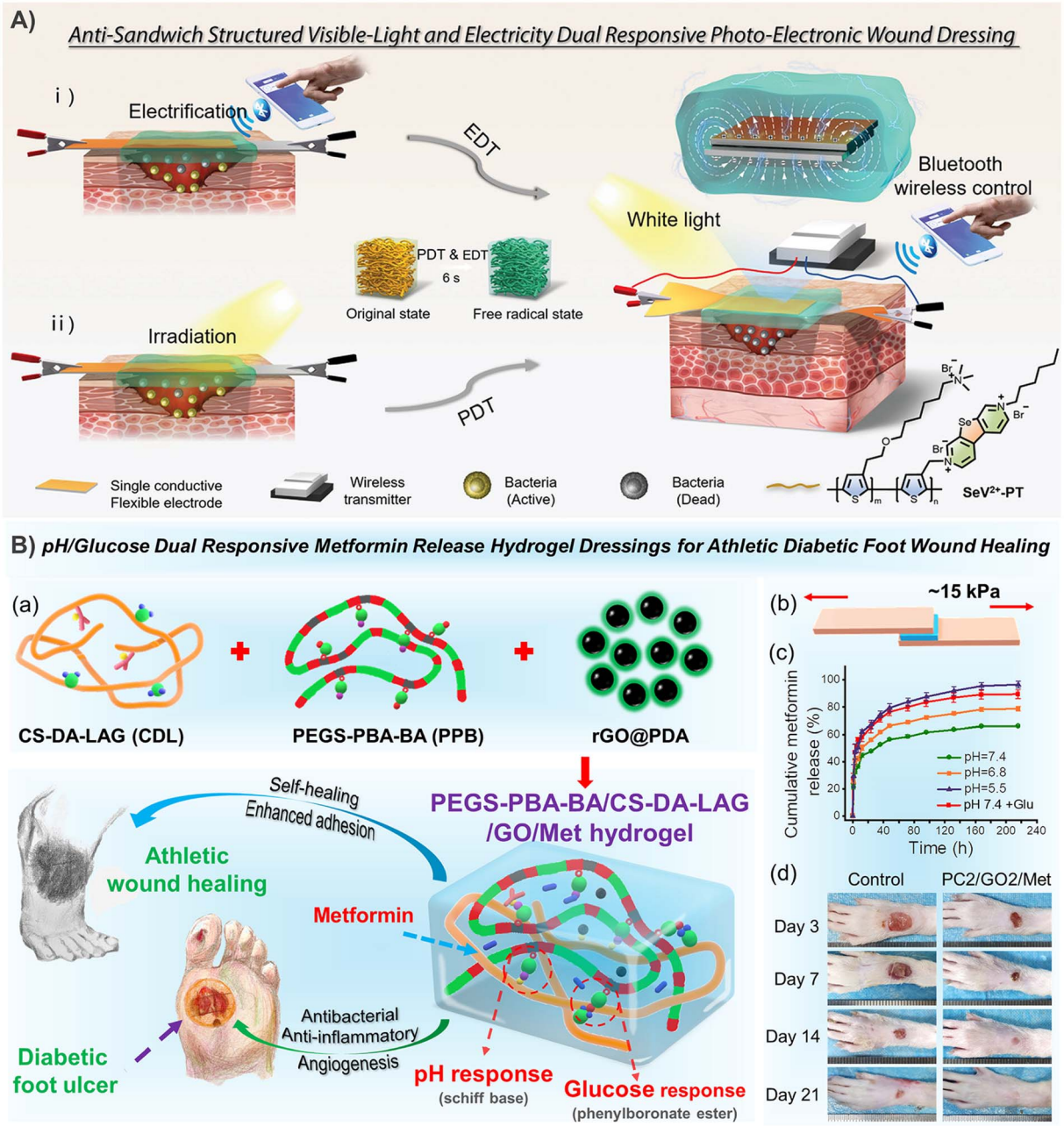

Fig. 7 CHs for skin repair. (A) The selenoviologen-appendant polythiophene (SeV^{2+}-PT)-containing polyacrylamide hydrogels rapidly generate renewable and stable ROS, which quickly and efficiently kills bacteria (6 s), and shortens the healing time of infected wounds to 7 days. Reproduced from ref. 90 with the permission of Wiley-VCH, copyright 2021. (B) Adhesion-enhanced phenylboronic acid, benzaldehyde bifunctional polyethylene glycol-*co*-poly(glycerol sebacic acid)/dihydrocaffeic acid and L-arginine co-grafted chitosan/polydopamine-coated reduced GO/Metformin (PEGS-PBA-BA/CS-DA-LAG/GO/Met) hydrogels with pH/glucose dual stimuli-responsive metformin release ability show a promoting effect on the healing of chronic athletic type II diabetic foot wounds. (a) Schematic diagram of hydrogel preparation and application. (b) Adhesion and (c) pH/glucose dual stimuli-responsive metformin release ability of the CHs. (d) Representative images of the rats' feet in the experimental and control groups during repair. Reproduced from ref. 21 with the permission of American Chemical Society, copyright 2022.

based on fast "click chemistry" and slow enzyme-mediated crosslinking. Specifically, the first CH network was rapidly formed by thiol–ene click reaction between hyperbranched poly(β-amino ester)-tetraaniline (PBAE-TA) and thiolated hyaluronic acid (HA-SH). Subsequently, vanillin-grafted gelatin (Geln-Van) and laccase (Lac) were added to the hydrogel through the Schiff base reaction to complete the second network. The finally prepared hydrogel can mediate the oxygen-consuming enzymatic reaction and up-regulate the expression of HIF-1α and connexin 43, and further promote angiogenesis, immune regulation, and the reconstruction of hair follicles and the dermal collagen matrix in diabetic rat wounds.[148] Deferoxamine (DFO), an FDA-approved iron chelating agent for the treatment of hemochromatosis, is also used to up-regulate the

expression of HIF-1α and the VEGF in diabetic wounds through pH-responsive release.[7] Other substances that are used to promote blood vessel regeneration also included exosomes.[149] In addition, in order to cope with the complex wounds caused by diabetes, CHs with continuous real-time monitoring of wound infection, mechanical strain, and blood glucose (Fig. 4C),[114] as well as intelligent management dressings integrating bionics, drug response release, wound secretion detection and motion sensing have also been reported (Fig. 11).[59] Especially for diabetic foot wounds, CHs combined with PDA@Ag and PANI not only promote angiogenesis, accelerate collagen deposition, and inhibit bacterial growth, but also have potential in epidermal sensors.[100] Furthermore, rGO@PDA-based CHs for pH/glucose dual-responsive release of metformin, a specific drug for type II diabetic foot wounds, have also been recently developed (Fig. 7B).[21]

It is well known that skin repair is divided into four phases: haemostasis, inflammation, proliferation and remodelling. According to the above studies, we can conclude that in the haemostasis phase, conductive hydrogels, especially ionic conductive hydrogels, can accelerate haemostasis by activating the coagulation pathway with their own electrical charge. In the inflammation phase, conductive materials facilitate the migration of macrophages and neutrophils, promote blood flow and tissue oxygenation, inhibit bacterial growth, reduce trauma oedema and play an antioxidant role. In the proliferation phase, conductive materials can promote wound contraction, enhance fibroblast proliferation, stimulate VEGF production by endothelial cells, promote angiogenesis and accelerate collagen deposition. In the remodeling phase, conductive hydrogels promote collagen maturation and remodeling (Fig. 6). In conclusion, in the past five years, CHs used for skin wound repair have shown great growth. However, skin wound repair is a complex and continuous process. There is still a long way to go for achieving morphologically perfect and functionally complete skin repair.

3.4 Bone repair

The mismatch between the modulus of conventional CHs and the ultra-high mechanical strength of bone tissue leads to the application of CHs in bone tissue repair and lags far behind that in other tissues, and the related research is also relatively small in amount. In one case, quaternized chitosan was used to prepare antibacterial scaffolds for bone tissue engineering.[150] On this basis, PANI was immobilized and introduced on a quaternized chitosan backbone by ammonium persulfate initiated *in situ* aniline polymerization. Subsequently, an injectable and self-healing CH was prepared with dextran oxide as the cross-linking agent.[78] In addition, the main osteogenic markers, such as ALP and calcium, were enhanced when the chitosan grafted PANI-based CHs were co-cultured with MC3T3-E1 cells.[151] When PANI is encapsulated in a GelMA hydrogel which can be printed by digital projection stereolithography, the CHs are proved to promote mineral deposition.[152] However, there is no significant difference in its ability to promote mineral deposition compared with the GelMA hydrogel. When PANI was prepared into fibers by electrospinning and then compounding with a hydrogel containing graphene, a hydrogel/fiber scaffold with conductivity in both a hydrogel and fiber was constructed. The experiment confirmed that the hydrogel/fiber composite was better than a hydrogel alone in supporting adhesion, proliferation and morphology of human osteoblast-like cells.[120] However, the *in vivo* biological toxicity of PANI must also be considered. In another hydrogel/fiber composite scaffold, CNTs were introduced as a nanofiber structure into an adenine/thymine functionalized heparin hydrogel, which was constructed by Watson–Crick base pairing. Compared with human adipose-derived stem cells (ASCs) cultured on the normal hydrogel, the spontaneous osteogenic ability of ASCs in the above CNT-based CH scaffold after combination with bone morphogenetic protein-2 (BMP-2) was 4 times higher.[153] In the further study of CNT-based CHs, the dispersion of CNTs was enhanced by PEG modification, and the incorporation of CNTs into a hydrogel after mixing with black phosphorus nanosheets was also confirmed to help bone tissue regeneration, because the *in situ* oxidation of phosphorus can produce stable release of phosphate.[49]

However, the above studies were all limited to *in vitro* and cellular-level tests. Therefore, the two recent studies further verified the potential of CHs to promote bone tissue regeneration in animal models. In one of the studies, β-CD-functionalized reduced GO (rGO) was used as a conductive component and mixed with a gelatin methacrylate (GM)/acryloyl-β-cyclodextrin (Ac-CD) based photo-crosslinked hydrogel. Subsequent studies also confirmed that the CHs accelerated the *in vivo* bone defect repair in a rat skull defect model by promoting collagen deposition and mineralization.[52] In another study, in order to cope with the decrease in autophagy in BMSCs derived from osteoporosis, rapamycin with an autophagy regulation function was added to the silver nanowire based CHs, which restored the decreased cell activity of BMSCs by up-regulating the autophagy level, thereby significantly improving bone integration, and inhibiting the infection in an osteoporosis environment *in vivo* through the antibacterial effect of silver (Fig. 8).[101]

In conclusion, most studies remain at a simple level to explore the effects of hydrogels on osteoblast differentiation, and still lack more practical cases of CHs in animal experiments of bone injury *in vivo*.

4. Mechanism of CHs promoting tissue repair

The introduction of conductive materials in a hydrogel has brought some special properties to make the CHs have better performance in promoting tissue repair. In this part, we will mainly discuss the role of the special properties of hydrogel dressings given by conductive materials in promoting tissue repair.

4.1 Anti-bacterial

In the process of wound repair, bacterial infection is always the biggest hidden danger hindering tissue repair, and this is often

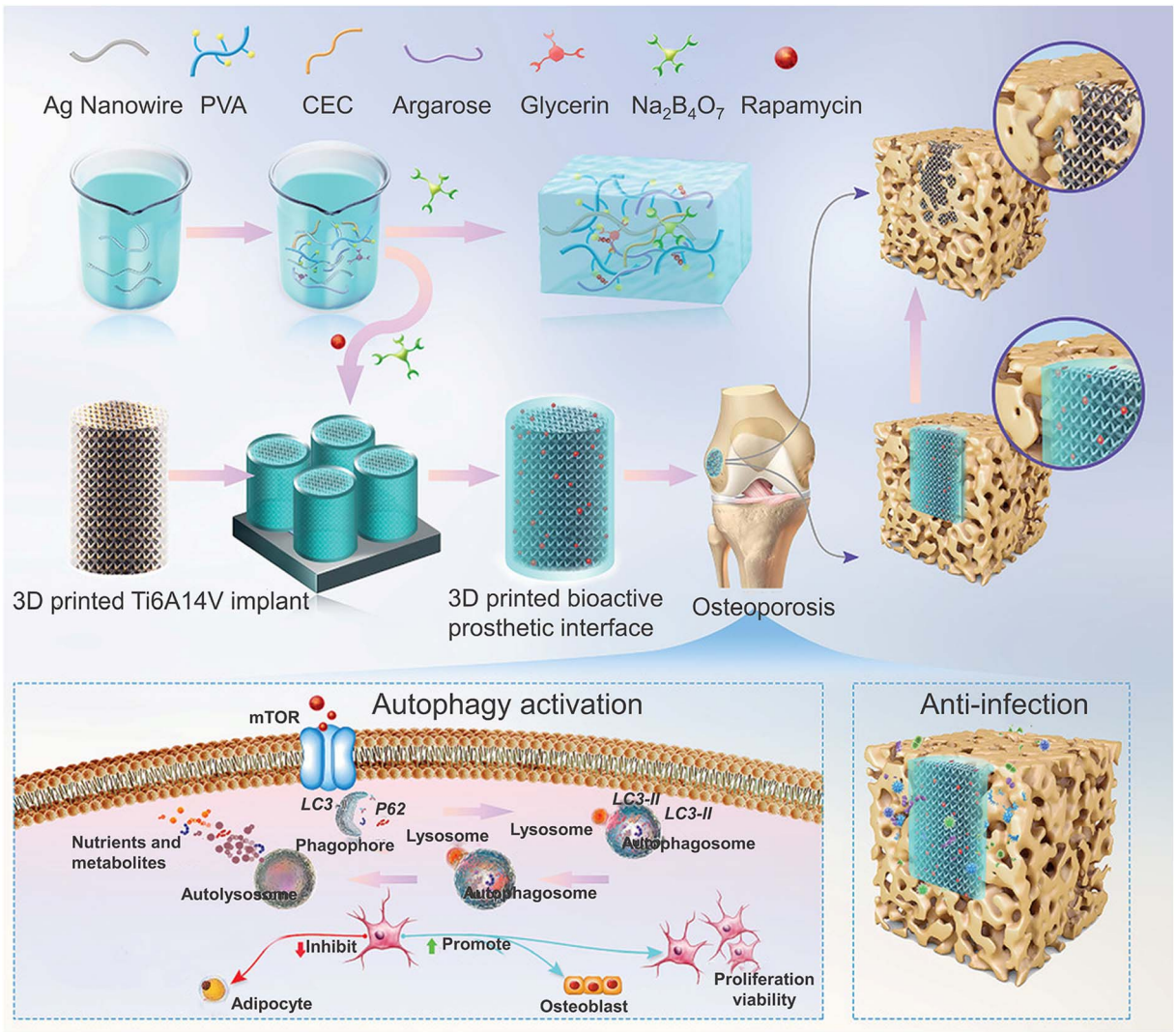

Fig. 8 CHs for bone repair. A rapamycin-loaded hydrogel restored the decreased cell activity of osteoporosis-derived BMSCs by up-regulating the autophagy level and showed excellent antibacterial activity against *S. aureus* and MRSA due to the silver nanowires. Reproduced from ref. 101 with the permission of Wiley-VCH, copyright 2022.

inevitable. Therefore, an antibacterial function in dressing is the most common solution strategy.[154] The natural characteristics of a hydrogel make it suitable for the delivery of antibiotics, which largely alleviates the abuse of antibiotics and reduces their dosage. So far, many antibiotics and antibacterial drugs have been encapsulated in CHs as sustained-release systems for local resistance to bacterial infection, such as amoxicillin,[23,76,142] vancomycin,[73] doxycycline,[20,39,40] moxifloxacin,[29] silver sulfadiazine,[24] *etc.* And metals, carbon-based materials, conductive polymers, and ionic compounds that can provide conductive properties to CHs can also provide antibacterial properties in different ways, which greatly promotes the rapid development of CHs. The most typical case is Ag, which not only shows good conductivity, but also provides excellent antibacterial properties to hydrogels,[101,102,123,155] and some silver-loaded antibacterial hydrogels have been used in clinical practice. In addition, the antibacterial activity of CNTs against many bacteria such as *Escherichia coli*, *Staphylococcus aureus*, *Staphylococcus mastoideus*, and *Bacillus subtilis* has been extensively studied because of their ability to disrupt bacterial cell membranes or increase the production of ROS.[156]

Most conductive materials, including metals like Ag, carbon-based materials like CNTs,[25,29,39] GO,[20,23,40,50–52] and conductive polymers such as PANI, PPy,[15,89] PEDOT *etc.*, have photothermal properties, which give hydrogels loaded with them photothermal antibacterial properties. In the study by He *et al.*, the Schiff base hydrogel based on *N*-carboxyethyl chitosan (CEC) and benzaldehyde terminated PF127 showed good photothermal antibacterial activity by using composite CNTs.[29] However, CNTs introduced by simple physical mixing have potential metabolic hazards. Therefore, the cross-linking between the dopamine modified on the CNT surface and the dopamine on the polymer in the hydrogel network solve the problems caused by physical mixing (Fig. 2A).[39] Similar operations can also be used for GO[40] and PPy.[89] Besides, the catechol group, the main skeleton of dopamine, has also been shown to

have a photothermal antibacterial effect when coordinated with Fe^{3+}.[143] And tannic acid with a similar structure is also considered to have an intrinsic antibacterial effect.[139] Similarly, some natural polymers have also been proved to have antibacterial activity. A typical one is chitosan, the only known cationic polysaccharide, and its antibacterial properties are also derived from its cationic properties,[77,116] as is polyethyleneimine.[57] In order to further increase the antibacterial properties of chitosan, cationic quaternary ammonium groups were also grafted on the main chain of chitosan.[7,20,50,78–80,143] On the other hand, grafting PANI or an aniline tetramer[75,77] on chitosan has also been shown to effectively enhance antibacterial properties,[7,78–80,142] which may result from the specific interaction of PANI with lipoteichoic acid to destroy the cell wall of Gram-positive bacteria.[147]

In addition, zwitterions such as poly[3-(dimethyl(4-vinylbenzyl) ammonium) propyl sulfonate][115] and ionic liquids such as 1-vinyl-3-(3-aminopropyl)-imidazolium tetrafluoroborate[10] were also used to prepare antibacterial CHs. In addition, some smart antibacterial conductive hydrogels have also been developed. Typically, in view of the responsiveness of hyaluronic acid to bacteria, hyaluronic acid-based ionic conductive hydrogels can achieve bacterial-responsive drug release. And CHs based on aniline trimer/polyaniline also provides an "on–off" precise drug control release system to achieve intelligent antibacterial properties.[74,142] In addition, the photothermal effect of graphene oxide was used to realize the responsive release of NO loaded in BNN6, and an intelligent controllable antibacterial strategy combining photothermal and gas therapy was realized.[51] In the study by Liang *et al.*, an intelligent synergistic strategy against complex drug-resistant bacterial infections was achieved by combining the inherent antibacterial properties of quaternary ammonium cations, the photothermal antibacterial properties of GO and the drug antibacterial properties provided by the sustained release of antibiotics (Fig. 9A).[20]

Overall, although many antibacterial strategies have been used to develop conductive tissue repair dressings, infection control is only the simplest step in tissue repair, and more complex repair processes require the synergy of other strategies. Further realization of real-time refined antibacterial response to the severity of bacterial infection is one of the possible development directions in the future.

4.2 Antioxidant and anti-inflammatory

In the process of tissue repair, excess ROS often greatly delays healing, leading to chronic wounds and even no healing. Therefore, the use of anti-inflammatory or antioxidant strategies to reduce excessive inflammation has been widely considered as a necessary strategy to promote tissue repair. The application of hydrogels with antioxidants[157] and inflammatory regulation[158] in chronic wounds has also been reviewed. By and large, the main way to achieve antioxidant function of these hydrogels is to be loaded with antioxidants (such as natural polyphenols, red jujube extract or modified polyphenols). For example, Qu *et al.* encapsulated curcumin with an antioxidant effect in benzaldehyde-terminated PF127 micelles through the amphiphilicity of PF127, and further crosslinked the micelles with quaternized chitosan through a Schiff base bond to prepare an antibacterial and antioxidant hydrogel.[159] The anti-inflammatory drug, diacerein, was loaded into CH containing CNTs to exert anti-inflammatory effects.[160] Another independent study also confirmed that diacerein-terminated four-arm polyethylene glycol and GO nanosheets can form antioxidant conductive supramolecular hydrogels through π–π stacking and hydrophobic interaction between GO and diacerein.[161] When tannic acid and recombinant human-like collagen were added to the dynamic cross-linking network of hydrogels composed of polyvinyl alcohol and borax, in addition to tannic acid, recombinant human-like collagen can also exert antioxidant effects.[139] However, these antioxidant hydrogels are difficult to be related to conductivity.

Interestingly, the electron transfer characteristics of conductive materials enable them to remove the excess free radicals that are generated during tissue repair, so as to play an antioxidant role. Therefore, antioxidant hydrogels based on conductive materials began to appear in some studies. For example, Zhao *et al.* grafted PANI onto quaternized chitosan and further combined it with aldehyde-modified polyester to form a Schiff base hydrogel, and they also confirmed for the first time that electron transfer or hydrogen atom donation of PANI fragments to DPPH radicals can achieve good antioxidant effects, which promote tissue repair (Fig. 3A).[79] Subsequent studies by the authors also found that aniline tetramers have the same effect.[76] Further study also confirmed that the addition of PPy nanotubes enhanced the antioxidant capacity (Fig. 5B)[88] of supramolecular hydrogels based on poly(*N*-isopropylacrylamide), quaternized chitosan-*graft*-β-cyclodextrin and adenine, which is due to their redox activity and nanotube structure.[146]

In addition, some studies have also combined conductive components with antioxidant components. For example, when CeO_2 nanoparticles with an antioxidant effect were uniformly deposited on Ti_3C_2Tx MXenes, the hydrogel containing it also has both antioxidant properties and conductivity (Fig. 2C).[57] Besides, the most typical case in this regard should be dopamine, which has antioxidant properties. Self-polymerization of dopamine under alkaline conditions can form a coating on the surface of CNTs,[39] GO (Fig. 9B),[40,41] MXenes,[60] *etc.*, which not only enhances the conductivity, water dispersibility and tissue adhesion of conductive materials, but also gives hydrogels based on the above conductive materials antioxidant properties. In another typical study, polydopamine (PDA) was used as a bridge to assemble PEDOT on the outer surface of silk microfibers, and an ultralong PEDOT coated PDA-functionalized silk microfibers (PEDOT-PDA-mSF) with a core-sheath structure were obtained. In this hydrogel, the electron capture ability of PDA can well eliminate ROS.[162] Similarly, conductive Ag-lignin nanoparticles were constructed, and a durable reduction–oxidation environment was formed inside the hydrogel through a dynamic redox system of catechol. This redox system that continuously produces catechol groups can also endow hydrogels with long-term and repeatable antioxidant properties and adhesion.[98,99]

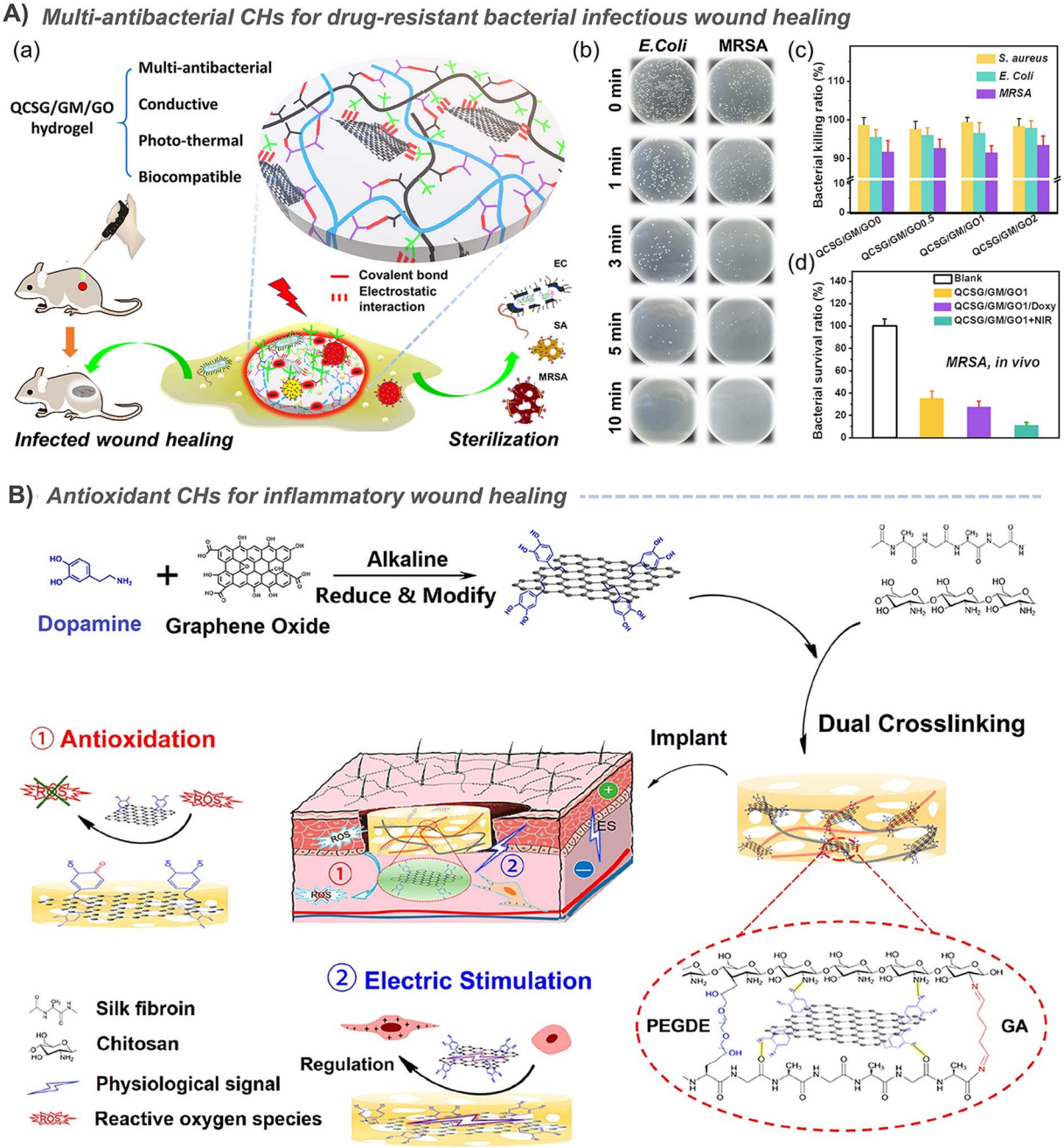

Fig. 9 (A) A synergistic strategy against complex drug-resistant bacterial infections by combining quaternary ammonium cationic antibacterial property, GO photothermal antibacterial property, and antibiotic sustained release antibacterial property. (a) Schematic diagram of hydrogel preparation and application. Tests results of (b) the *in vitro* photothermal antibacterial property, (c) quaternary ammonium cationic antibacterial property and (d) *in vivo* photothermal antibacterial property. Reproduced from ref. 20 with the permission of American Chemical Society, copyright 2020. (B) CHs containing polydopamine-coated reduced GO significantly scavenge ROS and promote the proliferation of C2C12 cells, thereby promoting skin wound healing. Reproduced from ref. 41 with the permission of American Chemical Society, copyright 2019.

In general, many CHs with antioxidant function have been used in tissue repair. But tissue repair is an extremely complex process and ROS also has many beneficial effects in the process of tissue repair, such as coordinating the recruitment of lymphocytes and mediating the defense of phagocytes. At the same time, it also can inhibit bacteria, and regulate angiogenesis and blood perfusion at the wound site. Therefore, considering the double-edged sword properties of ROS, direct and complete removal of ROS by application of conventional antioxidants does not effectively achieve regulation of inflammation in chronic wounds, as this may cause excessive reduction of ROS levels in target areas, surrounding tissues and/or blood vessels, thereby affecting the normal biological activity of ROS. Therefore, constructing ROS level-controlled responsive hydrogels to trigger intelligent responses may be an effective strategy to achieve controllable ROS elimination.

4.3 Stimulus response and intelligent delivery

The conductivity of CHs endows it with responsive characteristics to electrical stimulation, which also provides the possibility for stimuli-responsive material delivery.[63,163,164] For example, in a study by Guo *et al.*, CHs based on an aniline trimer generate a kind of "on–off" precise drug release system. When an additional voltage is applied, they can intelligently release more drugs for better tissue repair.[74] The reason for the electrically driven release of drug molecules in CHs is directly related to the EF driven migration of charged molecules, and the change of the overall net charge in the polymer during reduction or oxidation. Negatively charged drugs are released by reducing conductive polymers, while positively charged drugs are released by oxidation. In another work by our group, negatively charged amoxicillin and ibuprofen were incorporated into chitosan-*graft*-PANI/oxidized dextran hydrogels. After reduction of PANI, the positive charge in the hydrogel decreases, the drug molecules are expelled from the hydrogel, and the CHs shrink at the same time, which further accelerate the release of the drug.[142] The contraction of the same electrically conductive CNT hydrogel was also confirmed to promote the release of the neutral drug curcumin.[165] However, the operation of the external electric field is too complicated to facilitate use. Therefore, other stimuli-responsive CHs based on a dynamic wound environment were further developed.

In a typical example, PAM- and starch-based hydrogels integrated with triboelectric sensors can release BSA in a pH-mediated manner (pH range 4 to 10) because the swelling ratio of the PAM-based hydrogel decreases at lower pH values and the degradation rate of starch increases in low pH environments.[16] The reduction of electrostatic interactions in hydrogels based on anions and cations under acid and base conditions results in the release of polydopamine/Fe^{3+} nanoparticles loaded therein to scavenge ROS.[12] Besides, many self-healing CHs constructed from Schiff base structures can respond to pH changes[77,116,143,145] and release deferoxamine[7] and moxifloxacin hydrochloride,[29] at acidic pH. Similarly, hydrogels based on boric acid/phenylboronic acid and an o-diol structure also respond to pH.[25,155] However, wounds often only show a short acidic pH during acute inflammation, and most chronic wounds are alkaline, which should be paid attention to in the design of pH-responsive hydrogels in the future. In addition, the structure of phenylboronic acid ester is also responsive to glucose. For example, a polydopamine-reduced GO loaded CH based on Schiff base and phenylboronic acid ester double dynamic bonds between phenylboronic acid, benzaldehyde bifunctional polyethylene glycol-*co*-poly(glycerol sebacic acid)/dihydrocaffeic acid and L-arginine co-grafted chitosan can not only respond to the acidic pH during the acute inflammation period, but also respond to the high glucose environment in diabetic foot wounds, achieving local release of the type II diabetes-specific drug, metformin (Fig. 7B).[21] More specifically, the equilibrium of borate-based reactions can be adjusted by heating, ultrasonication, pH reduction and the introduction of diol-containing molecules. The diol group in the free molecule is more reactive than the PVA polymer. It can react with $Na_2B_4O_7$ as a competitor of PVA, leading to the release of rapamycin, promoting the up-regulation of autophagy in osteoporosis-derived BMSCs, and improving osseointegration (Fig. 8).[101] In another example, an electricity auto-generating glucose-responsive enzymatic-biofuel-cell (EBC) skin patch combines a glucose-responsive anodic enzyme (GDH, glucose dehydrogenase) and a cathodic counterpart (BOD, bilirubin oxidase). The electrons produced from GDH (grey) after response to the glucose reach BOD (blue) through the medium (yellow and green) and are eventually consumed for the oxygen reduction reaction. Through the completion of the redox reaction, the EBC system can produce about 400 mV of electricity with a maximum current density of about 10 $\mu A\ cm^{-2}$ (Fig. 10).[166] This is a novel method for preparing CHs. However, the continuity of the current generated in this way remains to be verified.

PNIPAM is a typical temperature-sensitive polymer, and PNIPAM-based hydrogels can respond to temperature to release drugs.[59] In one study, a graphene aerogel was first prepared by a freezing casting method, and then the polymerization of PDA NP containing *N*-isopropylacrylamide was initiated to prepare an interpenetrating binary network hydrogel. Because of the presence of graphene, the hydrogel can respond to infrared light to generate heat, which in turn triggers the thermal contraction of the NIPAM network,[36] achieving temperature or near-infrared light-controlled drug release.[38] A similar system containing graphene and PNIPAM can also assist wound closure, opening up a two-pronged wound management strategy by combining biomechanical and biochemical functions.[43] On the other hand, inspired by the thermosensitive properties of PNIPAN, a poly(*N*-isopropylacrylamide[166]-*co*-*n*-butyl acrylate[9])-poly(ethylene glycol)-poly(*N*-isopropylacrylamide[166]-*co*-*n*-butyl acrylate[9]) copolymer (denoted as PEP) was synthesized, which is gel-like at human temperature and becomes solution-like when the temperature become low. However, when the photothermal conductive silver nanoparticles modified reduced GO nanosheets (Ag@rGO) formed by *in situ* reduction of GO by silver ions were added to the above copolymer, the sol–gel reversibility at low temperature was well reversed, which was due to the strong synergistic coordination interactions between Ag@rGO nanosheets and the collapsed PNIPAM chains.[123] This study confirmed that Ag@rGO can reverse the effect of low temperature sol, which is of certain value in theory, but it is of little significance in practical application, when compared with conventional non-thermosensitive hydrogels. In addition, the corresponding CHs with photothermal,[29,40,51,89] photodynamic,[90] and sonodynamic functions can also respond to light and sound, respectively. For example, when the CHs containing β-cyclodextrin functionalized GO is combined with the nitric oxide donor BNN6, the photoelectric effect of GO and the temperature increase generated by its photothermal effect can promote BNN6 to produce NO and achieve a synergistic antibacterial effect of photothermal and gas therapy.[51] In addition, the decrease of the hydrogel's viscosity caused by light response also gives the dressing a good removability,[89,167] and the competitive binding of small molecules can also achieve this effect.[21,143]

Chronic wounds are often accompanied by excessive inflammation caused by excessive ROS production. So, a 3D printed CH strip based on an ionic liquid [2-(acryloyloxy) ethyl] trimethylammonium chloride and GelMA was combined with a doxycycline loaded ROS-responsive polyurethane membrane

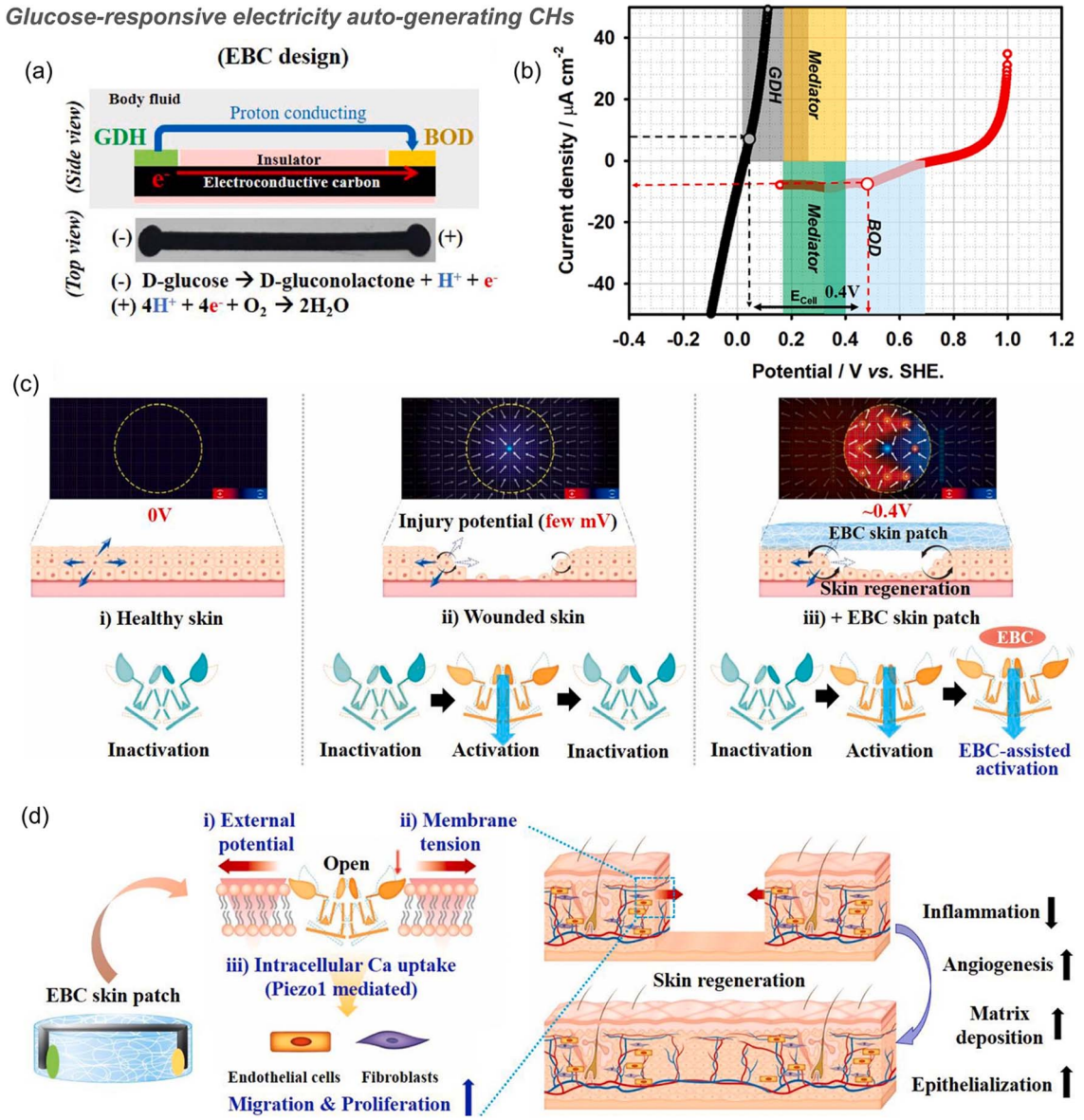

Fig. 10 Glucose-responsive electricity auto-generating enzymatic-biofuel-cell (EBC) skin patch for wound healing. (a) Schematic of the EBC patch that consists of the glucose-responsive anodic enzyme glucose dehydrogenase (GDH) and cathodic counterpart bilirubin oxidase (BOD) mounted on a conductive carbon strip. Taking glucose as the substrate, electrons produced by the GDH anode flow along the carbon strip and further react with protons, which are then converted to water at the BOD cathode. (b) When the maximum current density is about 10 μA cm^{-2}, the electrical potential generated by the EBC system is about 400 mV. (c) In the injured skin, an injury potential of about 25–45 mV was generated, which stimulated the opening of Piezo1, but with quick desensitization. When EBC was applied to induce an additional potential, a new potential distribution (~0.5 V) was generated, thereby slowing Piezo1 desensitization and increasing the intracellular calcium uptake. (d) Summary of activation events during wound healing induced by a EBC skin patch; the external potential generated by the EBC patch induces membrane tension, activates Piezo1 channel opening and calcium influx, and stimulates the activity and migration of ECs and FBs, which ultimately promote wound healing by enhancing angiogenesis, collagen deposition and re-epithelialization of injured tissues. Reproduced from ref. 166 with the permission of Elsevier, copyright 2021.

with a thioketal structure to prepare an antibacterial and anti-inflammatory dressing with ROS-responsive degradation and doxycycline release.[168] However, ROS also has a beneficial side, such as antibacterial properties, so that CHs that respond to light to produce ROS are also used to repair infected wounds (Fig. 7A).[90] MMP-2 and MMP-9 are also overexpressed in the inflammatory environment, so one study has combined the recombinant GST-tagged protein GST-TIMP-bFGF in the GSH-conjugated gelatin-based CHs. Gelatin in the hydrogel can be degraded by MMP, and TIMP (MMP substrate peptide) can also respond to MMP, which together promote the release of a basic fibroblast growth factor (bFGF) from the hydrogel, and ultimately enhance the functional recovery of the damaged spinal cord by promoting nerve regeneration and angiogenesis.[169]

In conclusion, many stimuli-responsive CHs have been used to deliver a variety of substances for tissue repair. However,

various parameters of the wound are dynamically changing during the repair process. It is still a great challenge to prepare CHs that can detect in real time and respond quickly.

4.4 Real-time monitoring

In consideration of the complexity of the tissue repair process and the real-time variability of various parameters in the wound, it is particularly important to monitor the wound state in real time, so that medical staff can make timely adjustments accordingly. Therefore, in order to understand the objective information of a wound environment, an intelligent dressing that can detect physiological markers (including temperature, pH, glucose concentration, lactic acid concentration and inflammatory cytokine levels) was recently proposed. Due to the excellent performance of CHs in biosensors, some CHs with real-time detection of the wound physiological state have also been developed. An obvious example is that the resistance of the CHs applied to the human body changes with tissue movement[25,122,170–172] or temperature changes.[16,36,173] For example, in a small pressure strain range, the pressure sensitivity of a hydrogel based on a polyvinyl alcohol/acrylamide-ionic liquid is as high as 9.18 kPa^{-1}. So, this hydrogel can accurately monitor various wound movements and small sharp stimuli. The electrical signal of the patient's movement can be transmitted to the nursing staff in real time to help the nursing staff find and deal with the patient's situation in time.[117] However, the importance of motion detection in the process of tissue repair is not very high. In further studies, changes in the stress, temperature, and exudates of the wound can all cause changes in the resistance of the polyacrylamide/starch double-network hydrogel. When a self-powered flexible triboelectric sensor is further integrated on the top of the hydrogel, it can also detect tactile signals with high precision.[16] However, this study was unable to distinguish which specific change was responsible for the change in resistance. So, a skin sensor system based on zwitterionic carboxyl betaine (SBMA) was constructed by Guo *et al.*, which introduced an insulating layer between the two hydrogel layers. Because of the temperature sensitivity of PNIPAM in the hydrogel, the upper layer hydrogel can respond to increased temperature, and then exclude excessive water through hydrophobic interaction, further increasing the ion concentration and causing the resistance to decrease; the lower layer hydrogel can respond to high glucose concentration through methylacrylamide phenylboric acid (MPBA), which also eventually leads to a decrease in resistance. The insulating layer in the middle ensures that the temperature and glucose signals do not interfere with each other. And the capacitance change of the whole hydrogel dressing can show the mechanical pressure of the wound. In summary, the above hydrogel dressing can continuously monitor and distinguish temperature, mechanical and glucose information in real time, and realize continuous real-time monitoring of infection, swelling and blood glucose in diabetic skin wounds (Fig. 4C).[114]

In another NIPAM-based thermosensitive drug release shark fin-like microneedle patch, researchers simultaneously constructed microfluidic channels on one side of the patch. With the help of capillary force, wound secretions and other liquids can pass through the channel without using any external power supply, and they finally reach the integrated detection area of an inverse opal photonic crystal (PC) structure. Using the fluorescence enhancement of PC, specific biomarkers in secretions can be sensitively detected by immunofluorescence assay. At the same time, a flexible electrode circuit is constructed on the other side of the patch, which can be used for motion sensing. After folding, a dressing integrating bionics, responsive drug release, wound secretion detection and motion sensing is formed for intelligent wound management (Fig. 11).[59] However, fluorescence detection is more restrictive and not an easy way to operate.

In general, the sensing properties of CHs make it possible to display changes in various parameters during wound healing, showing great prospects. However, at this stage, the distinguishing display of multiple parameters and continuous detection are still huge challenges needing to be further developed.

4.5 Promotion of cell proliferation and repair related pathway activation

As early as 2006, research by Zhao *et al.* confirmed that an endogenous EF can control the electrotaxis of cell migration in wound healing by affecting key signaling pathways such as PI3K/Pten (phosphoinositide 3-kinases/phosphatase and tensin homolog), membrane growth factor receptors and integrins.[2,3] Electrical stimulation (ES) can enhance the proliferation of fibroblasts and promote wound healing through the migration of the TGFβ1-ERK-NF-κB signaling pathway.[4] In addition, an external EF can stimulate endothelial cells to produce the VEGF[5] and activate PI3K-Akt and Rho-ROCK signaling pathways, thereby promoting angiogenesis in wound healing.[6,7] The combination of CHs containing Ag,[102] CNTs,[121] and MXenes ($Ti_3C_2T_X$),[61] with an ES significantly enhanced the proliferative activity of NIH3T3 cells. Some common phenomena are the promotion of neural stem cells (NSCs) in nerve repair,[28,46,81,109,127,131,174] cardiomyocytes in muscle repair,[33,37,55,106,110,133,175] NIH3T3 in skin repair,[61,102,121] and MC3T3 in bone repair.[49,52]

Taking the simple PPy-chitosan hydrogel as an example, the researchers confirmed that the CHs could reduce the tissue resistivity and susceptibility to arrhythmia, improve the electrical conduction velocity in the damage area, shorten the depolarization–repolarization time, and induce angiogenesis. These advantages make CHs retain cardiac function after myocardial infarction (MI) and they may provide treatment for cardiac resynchronization in patients with MI.[83] Further in-depth study found that PPy-based CHs can increase intracellular Ca^{2+}, which can induce cell proliferation and migration through Wnt/β-catenin and phosphatidylinositol 3-kinase (PI3K)/protein kinase B (Akt) and mitogen-activated protein kinase (MEK)/extracellular signal-regulated kinase (ERK) pathways (Fig. 12).[84,88,102,176] In diabetic wounds, PPy-based hydrogels combined with electrical stimulation enhance the expression of stress fibers and cell contractility in fibroblasts through the activation of Smad and Rac

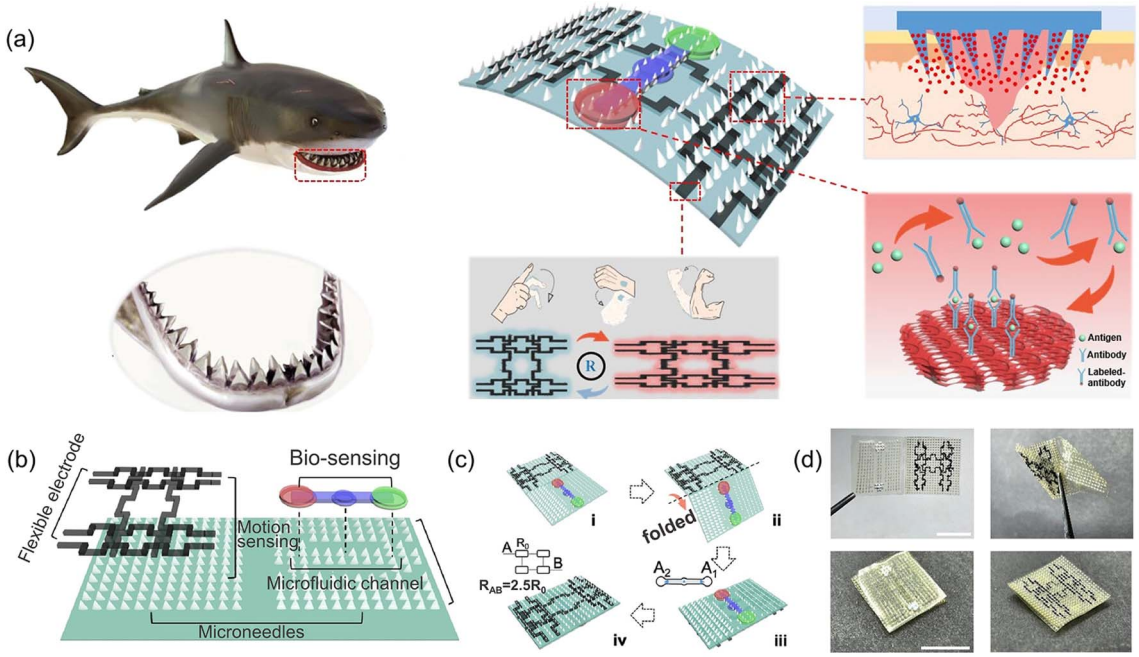

Fig. 11 CHs integrate bionics, responsive drug release, wound secretion detection and motion sensing for intelligent wound management. (a) Schematic diagram of shark tooth-inspired microneedle dressing for motion sensing, biochemical analysis, and healing. (b) Multifunctional microneedle dressing integrated with microfluidic channels and flexible electrodes. (c) Fabrication process of the origami multifunctional chip. (d) Image of the microneedle dressing before and after folding. Scale bar: 1 cm. Reproduced from ref. 59 with the permission of American Chemical Society, copyright 2021.

signaling pathways, as well as the protrusion of lamellipodia for cellular movement.[11]

CNT-containing hydrogels promote the diffusion and differentiation of NE-4C neural stem cells,[28] prolong the duration of cardiac action potential and induce bradycardia *in vivo* by reducing the activity of potassium channels in cardiac cells, while increasing the excitability of hippocampal CA1 neurons.[31] On the other hand, it can also promote the maturation and gap junction formation of cardiac cells, which may be due to its activation of ERK and RhoA pathways in cell development.[26]

Chitosan/silk fibroin hydrogel containing polydopamine-coated reduced GO can significantly promote the proliferation of C2C12 cells and the formation and length of pseudopods under electrical stimulation, and the cells have a high aspect ratio on the electroactive scaffold, thereby promoting skin wound healing (Fig. 9B).[41] EDC/NHS crosslinked amino graphene/collagen cryogels have been shown to support stemness and neuronal differentiation of BM-MSCs under electrical stimulation, increase CD90 and CD73 gene expression and paracrine ATP, and increase IDO activity of BM-MSCs, thereby supporting immunomodulatory function.[45]

An electricity auto-generating glucose-responsive enzymatic-biofuel-cell (EBC) skin patch can accelerate wound healing by modulating inflammation while stimulating angiogenesis, fibroblast functionality and matrix synthesis. And further research also testified that EBC-activated cellular behaviors were linked to the signaling involved with the calcium influx, which was predominantly dependent on the mechanosensitive ion channels, primarily Piezo1 (Fig. 10).[166] In addition, HIF-1α, VEGF and ANG-1 were significantly up-regulated, indicating that hypoxia-induced CHs play an important role in stimulating ADSCs to continuously secrete a variety of pro-angiogenic factors.[148] And the ionic liquid-based ROS-responsive release of doxycycline CHs has been shown to promote endothelial cell migration and macrophage polarization to the anti-inflammatory phenotype (M2) *in vitro*.[168] Compared with the cardiomyocytes in the hydrogel embedded with an electronic conductor, the cardiomyocytes cultured in the PAA composited hydrogel showed more orientation and elongated sarcomeres.[110] In conclusion, some explorations have been carried out to try to figure out how conductive materials affect the process of tissue repair. However, the human body is a complex system, and repair is a process that relies on the intricate synergy between a series of highly regulated factors. Therefore, further in-depth research is still significant, and it is also of great value to guide the preparation of new CHs.

5. Conclusion and outlook

Apparently perfect and function integrity tissue repair is an important issue in the biomedical field. CHs, which combine the electrophysiological characteristics of conductive materials and the flexible 3D bionic network of hydrogels, have shown great advantages in recent studies. CHs based on carbon-based conductive materials, organic conductive polymers, inorganic conductive metals, and ionic compounds have been widely developed to repair tissues such as nerves, muscles, skin, and bone. However, there are still great challenges.

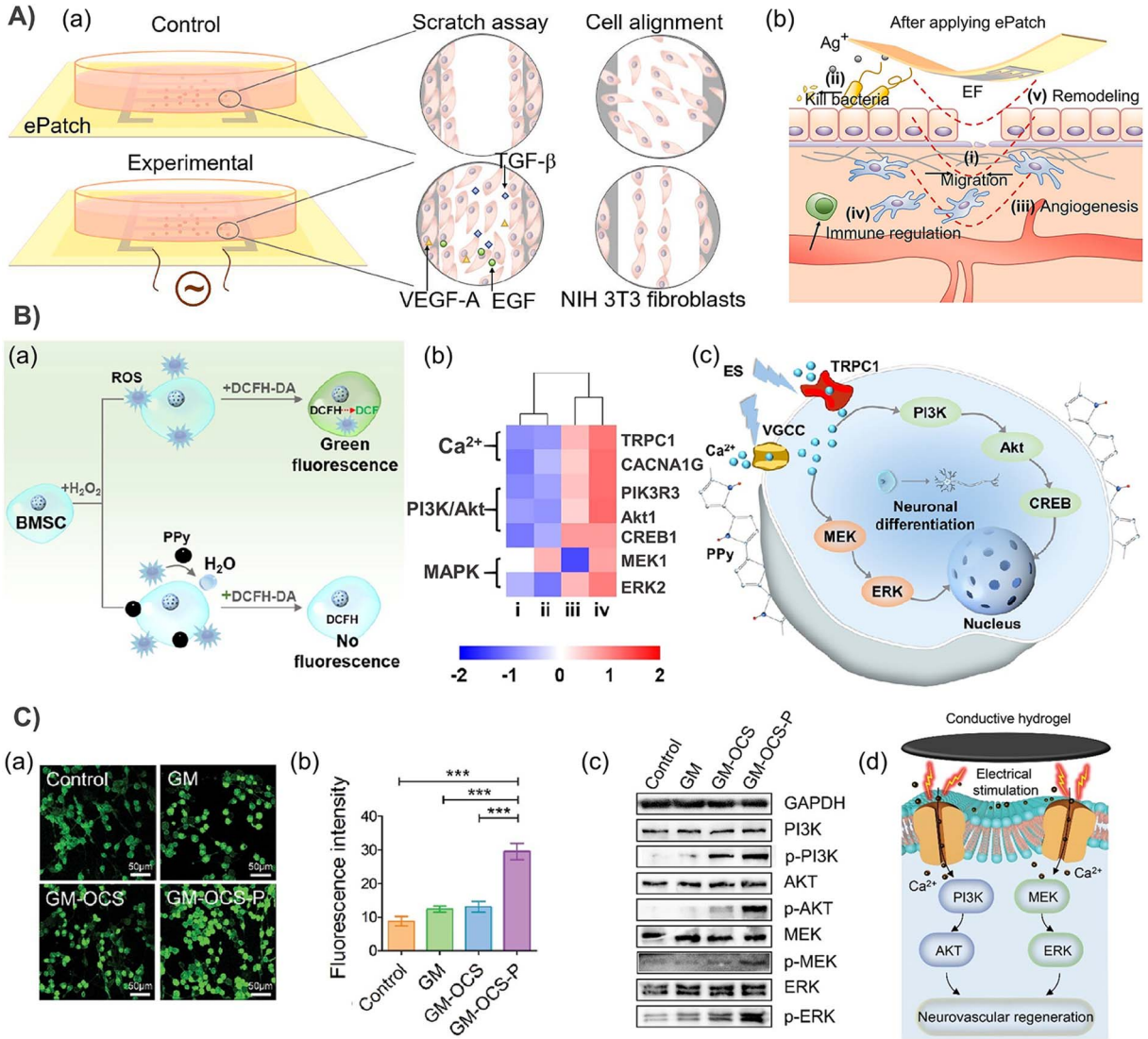

Fig. 12 (A) (a) A schematic diagram for testing EF-responsive cell behavior changes. (b) Schematic diagram of an ePatch promoting wound repair by (i) accelerating fibroblast migration and proliferation; (ii) inhibiting bacterial growth; (iii) promoting angiogenesis; (iv) down-regulation of immune cell activity; and (v) improving re-epithelialization and tissue remodeling. Reproduced from ref. 102 with the permission of Elsevier, copyright 2022. (B) (a) PPy embedded hydrogel downgrades the intracellular ROS level. (b) Heat map of genes related to the Ca^{2+} channel, PI3K/Akt pathway and MAPK pathway. (i–iv) denote CHP0, CHP0 + ES, CHP0.5, and CHP0.5 + ES, respectively. (c) A schematic diagram of enhanced conductivity and an ES promoting neuronal differentiation of BMSCs. Reproduced from ref. 88 with the permission of American Chemical Society, copyright 2021. (C) (a) Immunofluorescence staining of intracellular Ca^{2+} in PC12 cells. (b) Quantitative statistics of the intracellular Ca^{2+} concentration in different treatment groups. (c) The protein expressions of PI3K, p-PI3K, AKT, p-AKT, MEK, p-MEK, ERK, and p-ERK were evaluated by western blot. (d) Mechanism diagram of CHs promoting neurovascular regeneration. Reproduced from ref. 84 with the permission of Wiley-VCH, copyright 2022.

First and foremost, as a biomedical material, the feasibility of achieving clinical translation is the gold standard for CH evaluation. However, most of the electroactive components that can be used to construct CHs have potential toxicity, which needs to be highly valued in future research. In addition, to perfectly meet the needs of tissue repair, the current CHs still have great challenges in freely adjustable mechanical properties. Typically, the preparation of high strength hydrogels suitable for bone tissue repair still has great difficulties. And when further facing chronic wounds, the threat of drug-resistant bacteria, the balance of excessive inflammation, the elimination of the effects of underlying diseases, and the psychological state of patients are all areas that need further exploration. Besides, there are many factors affecting the conductivity of conductive hydrogels *in vivo*. How to achieve performance stability and standardization is also a huge problem affecting its clinical transformation. Therefore, exploration in this field is also necessary. Recently, some reports of electricity auto-generating hydrogel dressings have further enriched the CH family by combining triboelectric nanogenerators[12–17] or glucose-responsive enzymatic-biofuel-cells.[166] This may be a direction for future research, because it

greatly enhanced the electrical signals at the wound and improves the deficiency of weak current in an endogenous EF. Moreover, ethical issues have to be considered in the translation of biomaterials, which mainly makes it difficult to carry out clinical studies.

Secondly, to understand the state of real-time changes in complex wounds and make corresponding treatment in time, tissue repair monitoring based on CHs has been proposed and is still in the preliminary exploration stage. Most of the research still stays in the simple combination of sensors and hydrogels or the detection of a single parameter, and hydrogel sensors with multi-parameter separation detection are still lacking. In the subsequent exploration of multi-parameter separation detection, the potential problems of signal coupling and crosstalk are the key to translational applications. This may be solved by analyzing the subtle signal characteristics and the modular design of the device, which are divided into several functional subareas and each responds to a specific stimulus. In the future, a integrated, programmatic and automated CH dressing that combines detection, analysis and intervention or treatment may enable a high level of intelligent wound care with improved accuracy and efficacy.

Thirdly, excessive inflammation is the main cause of long-term nonunion of tissue damage, and current conductive hydrogels mainly solve this problem through anti-inflammation. However, inflammation is a double-edged sword, and too low inflammation may also hinder tissue repair, so further exploration of intelligent inflammation regulation strategies is also a future development direction of conductive hydrogels. At the same time, exploring the influence of conductivity on inflammation, and then trying to regulate inflammation by electrical stimulation or self-regulation of inflammation by an electrical response is also a possible effective way.

Finally, although some molecular mechanisms of electrical stimulation promoting tissue repair have been studied, there is still a lack of further molecular and signaling studies on how conductive materials affect tissue repair processes. In other words, it is necessary to further explore the relationship between conductive materials and electrical stimulation, and how they interact in promoting tissue repair.

In general, the application of conductive materials in tissue repair is only beginning to emerge. We expect that more functional CHs can be explored for tissue repair and even wound monitoring in the future, and also expect more CHs to come out of the laboratory and be applied in clinical practice.

Author contributions

The manuscript was written through the contributions of all authors. All authors have given approval to the final version of the manuscript.

Conflicts of interest

There are no conflicts to declare.

Acknowledgements

This work was jointly supported by the National Natural Science Foundation of China (No. 51973172 and 52273149), the Natural Science Foundation of Shaanxi Province (No. 2020JC-03), the State Key Laboratory for Mechanical Behavior of Materials, the World-Class Universities (Disciplines) and Characteristic Development Guidance Funds for the Central Universities, and China Postdoctoral Science Foundation (2022M712498).

References

1 N. Nguyen, Z.-H. Lin, S. R. Barman, C. Korupalli, J.-Y. Cheng, N.-X. Song, Y. Chang, F.-L. Mi, H.-L. Song, H.-W. Sung and Y.-J. Lin, *Nano Energy*, 2022, **99**, 107393.
2 M. Zhao, *Semin. Cell Dev. Biol.*, 2009, **20**, 674–682.
3 M. Zhao, B. Song, J. Pu, T. Wada, B. Reid, G. Tai, F. Wang, A. Guo, P. Walczysko, Y. Gu, T. Sasaki, A. Suzuki, J. V. Forrester, H. R. Bourne, P. N. Devreotes, C. D. McCaig and J. M. Penninger, *Nature*, 2006, **442**, 457–460.
4 Y. Wang, M. Rouabhia and Z. Zhang, *Biochim. Biophys. Acta, Gen. Subj.*, 2016, **1860**, 1551–1559.
5 M. Zhao, H. Bai, E. Wang, J. V. Forrester and C. D. McCaig, *J. Cell Sci.*, 2004, **117**, 397–405.
6 R. Luo, J. Dai, J. Zhang and Z. Li, *Adv. Healthcare Mater.*, 2021, **10**, 2100557.
7 C. Wu, L. Long, Y. Zhang, Y. Xu, Y. Lu, Z. Yang, Y. Guo, J. Zhang, X. Hu and Y. Wang, *J. Controlled Release*, 2022, **344**, 249–260.
8 H. Huang, Z. Dong, X. Ren, B. Jia, G. Li, S. Zhou, X. Zhao and W. Wang, *Nano Res.*, 2023, **16**, 3475–3515.
9 J. T. Peters, M. E. Wechsler and N. A. Peppas, *Regener. Biomater.*, 2021, **8**, rbab060.
10 P. Liu, K. Jin, W. Wong, Y. Wang, T. Liang, M. He, H. Li, C. Lu, X. Tang, Y. Zong and C. Li, *Chem. Eng. J.*, 2021, **415**, 129025.
11 Y. Lu, Y. Wang, J. Zhang, X. Hu, Z. Yang, Y. Guo and Y. Wang, *Acta Biomater.*, 2019, **89**, 217–226.
12 R. Yuan, N. Yang, S. Fan, Y. Huang, D. You, J. Wang, Q. Zhang, C. Chu, Z. Chen, L. Liu and L. Ge, *Small*, 2021, **17**, 2103997.
13 S. Du, N. Zhou, Y. Gao, G. Xie, H. Du, H. Jiang, L. Zhang, J. Tao and J. Zhu, *Nano Res.*, 2020, **13**, 2525–2533.
14 S.-H. Jeong, Y. Lee, M.-G. Lee, W. J. Song, J.-U. Park and J.-Y. Sun, *Nano Energy*, 2021, **79**, 105463.
15 S. Du, H. Suo, G. Xie, Q. Lyu, M. Mo, Z. Xie, N. Zhou, L. Zhang, J. Tao and J. Zhu, *Nano Energy*, 2022, **93**, 106906.
16 X. Lin, Y. Mao, P. Li, Y. Bai, T. Chen, K. Wu, D. Chen, H. Yang and L. Yang, *Adv. Sci.*, 2021, **8**, 2004627.
17 X. Xiao, X. Xiao, A. Nashalian, A. Libanori, Y. Fang, X. Li and J. Chen, *Adv. Healthcare Mater.*, 2021, **10**, 2100975.
18 R. Eivazzadeh-Keihan, E. Bahojb Noruzi, E. Chidar, M. Jafari, F. Davoodi, A. Kashtiaray, M. Ghafori Gorab, S. Masoud Hashemi, S. Javanshir, R. Ahangari Cohan, A. Maleki and M. Mahdavi, *Chem. Eng. J.*, 2022, **442**, 136183.

19 J. Anjali, V. K. Jose and J.-M. Lee, *J. Mater. Chem. A*, 2019, **7**, 15491–15518.
20 Y. Liang, B. Chen, M. Li, J. He, Z. Yin and B. Guo, *Biomacromolecules*, 2020, **21**, 1841–1852.
21 Y. Liang, M. Li, Y. Yang, L. Qiao, H. Xu and B. Guo, *ACS Nano*, 2022, **16**, 3194–3207.
22 F. Zheng, R. Li, Q. He, K. Koral, J. Tao, L. Fan, R. Xiang, J. Ma, N. Wang, Y. Yin, Z. Huang, P. Xu and H. Xu, *Mater. Sci. Eng., C*, 2020, **109**, 110560.
23 S. Wang, W. Zhang, J. Yan, G. Meng, L. Cui, W. Li, Z. Liu and X. Guo, *Macromol. Mater. Eng.*, 2022, **307**, 2100878.
24 M. U. A. Khan, S. Haider, M. A. Raza, S. A. Shah, S. I. Abd Razak, M. R. A. Kadir, F. Subhan and A. Haider, *Int. J. Biol. Macromol.*, 2021, **192**, 820–831.
25 G. Xiao, Y. Wang, H. Zhang, Z. Zhu and S. Fu, *Int. J. Biol. Macromol.*, 2021, **170**, 272–283.
26 R. Bai, J. Liu, J. Zhang, J. Shi, Z. Jin, Y. Li, X. Ding, X. Zhu, C. Yuan, B. Xiu, H. Liu, Z. Yuan and Z. Liu, *J. Nanobiotechnol.*, 2021, **19**, 252.
27 S.-Y. Park, J.-H. Kang, H.-S. Kim, J.-Y. Hwang and U. S. Shin, *Nanoscale*, 2022, **14**, 2367–2382.
28 M. Xu, Q. Li, Z. Fang, M. Jin, Q. Zeng, G. Huang, Y.-G. Jia, L. Wang and Y. Chen, *Biomater. Sci.*, 2020, **8**, 6957–6968.
29 J. He, M. Shi, Y. Liang and B. Guo, *Chem. Eng. J.*, 2020, **394**, 124888.
30 A. N. Koppes, K. W. Keating, A. L. McGregor, R. A. Koppes, K. R. Kearns, A. M. Ziemba, C. A. McKay, J. M. Zuidema, C. J. Rivet, R. J. Gilbert and D. M. Thompson, *Acta Biomater.*, 2016, **39**, 34–43.
31 P. C. Sherrell, A. Cieslar-Pobuda, M. S. Ejneby, L. Sammalisto, A. Gelmi, E. de Muinck, J. Brask, M. J. Los and M. Rafat, *Macromol. Biosci.*, 2017, **17**, 1600446.
32 B. Liu, Y. Wang, Y. Miao, X. Zhang, Z. Fan, G. Singh, X. Zhang, K. Xu, B. Li, Z. Hu and M. Xing, *Biomaterials*, 2018, **171**, 83–96.
33 L. Wang, Y. Liu, G. Ye, Y. He, B. Li, Y. Guan, B. Gong, K. Mequanint, M. M. Q. Xing and X. Qiu, *Nat. Biomed. Eng.*, 2021, **5**, 1157–1173.
34 X. Li, X. Huang, H. Mutlu, S. Malik and P. Theato, *Soft Matter*, 2020, **16**, 10969–10976.
35 R. Bao, B. Tan, S. Liang, N. Zhang, W. Wang and W. Liu, *Biomaterials*, 2017, **122**, 63–71.
36 M. Zhang, F. Deng, L. Tang, H. Wu, Y. Ni, L. Chen, L. Huang, X. Hu, S. Lin and C. Ding, *Chem. Eng. J.*, 2021, **405**, 126756.
37 J. Zhou, X. Yang, W. Liu, C. Wang, Y. Shen, F. Zhang, H. Zhu, H. Sun, J. Chen, J. Lam, A. G. Mikos and C. Wang, *Theranostics*, 2018, **8**, 3317–3330.
38 Y. Zhu, Q. Zeng, Q. Zhang, K. Li, X. Shi, F. Liang and D. Han, *Nanoscale*, 2020, **12**, 8679–8686.
39 Y. Liang, X. Zhao, T. Hu, Y. Han and B. Guo, *J. Colloid Interface Sci.*, 2019, **556**, 514–528.
40 Y. P. Liang, X. Zhao, T. L. Hu, B. J. Chen, Z. H. Yin, P. X. Ma and B. L. Guo, *Small*, 2019, **15**, 1900046.
41 P. Tang, L. Han, P. Li, Z. Jia, K. Wang, H. Zhang, H. Tan, T. Guo and X. Lu, *ACS Appl. Mater. Interfaces*, 2019, **11**, 7703–7714.
42 L. Yan, T. Zhou, L. Han, M. Zhu, Z. Cheng, D. Li, F. Ren, K. Wang and X. Lu, *Adv. Funct. Mater.*, 2021, **31**, 2010465.
43 M. Li, Y. Liang, J. He, H. Zhang and B. Guo, *Chem. Mater.*, 2020, **32**, 9937–9953.
44 M. Izadifar, D. Chapman, P. Babyn, X. Chen and M. E. Kelly, *Tissue Eng., Part C*, 2018, **24**, 74–88.
45 G. Agarwal, N. Kumar and A. Srivastava, *Mater. Sci. Eng., C*, 2021, **118**, 111518.
46 S.-J. Lee, W. Zhu, M. Nowicki, G. Lee, H. Dong Nyoung, J. Kim, Y. Y. Zuo and L. G. Zhang, *J. Neural Eng.*, 2018, **15**, 016018.
47 X. Liu, A. L. Miller II, S. Park, B. E. Waletzki, A. Terzic, M. J. Yaszemski and L. Lu, *J. Mater. Chem. B*, 2016, **4**, 6930–6941.
48 L. Sang, Y. Liu, W. Hua, K. Xu, G. Wang, W. Zhong, L. Wang, S. Xu, M. M. Q. Xing and X. Qiu, *RSC Adv.*, 2016, **6**, 26341–26351.
49 X. Liu, M. N. George, L. Li, D. Gamble, A. L. Miller Ii, B. Gaihre, B. E. Waletzki and L. Lu, *ACS Biomater. Sci. Eng.*, 2020, **6**, 4653–4665.
50 B. Zhang, J. He, M. Shi, Y. Liang and B. Guo, *Chem. Eng. J.*, 2020, **400**, 125994.
51 S. Huang, H. Liu, K. Liao, Q. Hu, R. Guo and K. Deng, *ACS Appl. Mater. Interfaces*, 2020, **12**, 28952–28964.
52 Y. Li, J. He, J. Zhou, Z. Li, L. Liu, S. Hu, B. Guo and W. Wang, *Biomater. Sci.*, 2022, **10**, 1326–1341.
53 X. Zhao, Z. Zhang, J. Luo, Z. Wu, Z. Yang, S. Zhou, Y. Tu, Y. Huang, Y. Han and B. Guo, *Appl. Mater. Today*, 2022, **26**, 101365.
54 M. Tashakori-Miyanroudi, K. Rakhshan, M. Ramez, S. Asgarian, A. Janzadeh, Y. Azizi, A. Seifalian and F. Ramezani, *Int. J. Biol. Macromol.*, 2020, **163**, 1136–1146.
55 R. Si, C. Gao, R. Guo, C. Lin, J. Li and W. Guo, *J. Photochem. Photobiol., B*, 2020, **206**, 111789.
56 Y.-Z. Zhang, J. K. El-Demellawi, Q. Jiang, G. Ge, H. Liang, K. Lee, X. Dong and H. N. Alshareef, *Chem. Soc. Rev.*, 2020, **49**, 7229–7251.
57 H. Zheng, S. Wang, F. Cheng, X. He, Z. Liu, W. Wang, L. Zhou and Q. Zhang, *Chem. Eng. J.*, 2021, **424**, 130148.
58 L. Zhou, H. Zheng, Z. Liu, S. Wang, Z. Liu, F. Chen, H. Zhang, J. Kong, F. Zhou and Q. Zhang, *ACS Nano*, 2021, **15**, 2468–2480.
59 M. Guo, Y. Wang, B. Gao and B. He, *ACS Nano*, 2021, **15**, 15316–15327.
60 G. Ye, Z. Wen, F. Wen, X. Song, L. Wang, C. Li, Y. He, S. Prakash and X. Qiu, *Theranostics*, 2020, **10**, 2047–2066.
61 L. Mao, S. Hu, Y. Gao, L. Wang, W. Zhao, L. Fu, H. Cheng, L. Xia, S. Xie, W. Ye, Z. Shi and G. Yang, *Adv. Healthcare Mater.*, 2020, **9**, 2000872.
62 T.-C. Sun, X.-C. Ning, S. Ramakrishna, Y.-Z. Long and J. Zhang, *Chem. Eng. J.*, 2022, **453**, 139667.
63 Z. Deng, R. Yu and B. Guo, *Mater. Chem. Front.*, 2021, **5**, 2092–2123.
64 C. Yu, F. Yao and J. Li, *Acta Biomater.*, 2022, **139**, 4–21.
65 T. Nezakati, A. Seifalian, A. Tan and A. M. Seifalian, *Chem. Rev.*, 2018, **118**, 6766–6843.

66 B. L. Guo and P. X. Ma, *Biomacromolecules*, 2018, **19**, 1764–1782.
67 B. Guo, L. Glavas and A.-C. Albertsson, *Prog. Polym. Sci.*, 2013, **38**, 1263–1286.
68 Y. Wu, L. Wang, B. Guo, Y. Shao and P. X. Ma, *Biomaterials*, 2016, **87**, 18–31.
69 J. Chen, B. Guo, T. W. Eyster and P. X. Ma, *Chem. Mater.*, 2015, **27**, 5668–5677.
70 M. Xie, L. Wang, B. Guo, Z. Wang, Y. E. Chen and P. X. Ma, *Biomaterials*, 2015, **71**, 158–167.
71 M. Xie, L. Wang, J. Ge, B. Guo and P. X. Ma, *ACS Appl. Mater. Interfaces*, 2015, **7**, 6772–6781.
72 T. L. Hu, Y. B. Wu, X. Zhao, L. Wang, L. Y. Bi, P. X. Ma and B. L. Guo, *Chem. Eng. J.*, 2019, **366**, 208–222.
73 M. Li, J. Chen, M. T. Shi, H. L. Zhang, P. X. Ma and B. L. Guo, *Chem. Eng. J.*, 2019, **375**, 121999.
74 J. Qu, Y. P. Liang, M. T. Shi, B. L. Guo, Y. Z. Gao and Z. H. Yin, *Int. J. Biol. Macromol.*, 2019, **140**, 255–264.
75 B. Guo, J. Qu, X. Zhao and M. Zhang, *Acta Biomater.*, 2019, **84**, 180–193.
76 J. Qu, X. Zhao, Y. P. Liang, Y. M. Xu, P. X. Ma and B. L. Guo, *Chem. Eng. J.*, 2019, **362**, 548–560.
77 R. Dong, X. Zhao, B. Guo and P. X. Ma, *ACS Appl. Mater. Interfaces*, 2016, **8**, 17138–17150.
78 X. Zhao, P. Li, B. Guo and P. X. Ma, *Acta Biomater.*, 2015, **26**, 236–248.
79 X. Zhao, H. Wu, B. Guo, R. Dong, Y. Qiu and P. X. Ma, *Biomaterials*, 2017, **122**, 34–47.
80 Y. Wu, Y. Lu, C. Wu, J. Chen, N. Ning, Z. Yang, Y. Guo, J. Zhang, X. Hu and Y. Wang, *J. Mater. Chem. B*, 2021, **9**, 8138–8146.
81 J. Xu, C.-W. Wong and S.-H. Hsu, *Chem. Mater.*, 2020, **32**, 10407–10422.
82 D. Gan, L. Han, M. Wang, W. Xing, T. Xu, H. Zhang, K. Wang, L. Fang and X. Lu, *ACS Appl. Mater. Interfaces*, 2018, **10**, 36218–36228.
83 S. He, J. Wu, S.-H. Li, L. Wang, Y. Sun, J. Xie, D. Ramnath, R. D. Weisel, T. M. Yau, H.-W. Sung and R.-K. Li, *Biomaterials*, 2020, **258**, 120285.
84 L. Fan, C. Xiao, P. Guan, Y. Zou, H. Wen, C. Liu, Y. Luo, G. Tan, Q. Wang, Y. Li, P. Yu, L. Zhou and C. Ning, *Adv. Healthcare Mater.*, 2022, **11**, 2101556.
85 S. Liang, Y. Zhang, H. Wang, Z. Xu, J. Chen, R. Bao, B. Tan, Y. Cui, G. Fan, W. Wang, W. Wang and W. Liu, *Adv. Mater.*, 2018, **30**, 1704235.
86 Y. Bu, H.-X. Xu, X. Li, W.-J. Xu, Y.-X. Yin, H.-L. Dai, X.-B. Wang, Z.-J. Huang and P.-H. Xu, *RSC Adv.*, 2018, **8**, 10806–10817.
87 X. Wang, X. Li, L. Zhao, M. Li, Y. Li, W. Yang and J. Ren, *Soft Matter*, 2021, **17**, 8363–8372.
88 C. Wu, S. Chen, T. Zhou, K. Wu, Z. Qiao, Y. Zhang, N. Xin, X. Liu, D. Wei, J. Sun, H. Luo, L. Zhou and H. Fan, *ACS Appl. Mater. Interfaces*, 2021, **13**, 52346–52361.
89 L. Feng, W. Shi, Q. Chen, H. Cheng, J. Bao, C. Jiang, W. Zhao and C. Zhao, *Adv. Healthcare Mater.*, 2021, **10**, 2100784.
90 K. Zhou, D. Chigan, L. Xu, C. Liu, R. Ding, G. Li, Z. Zhang, D. Pei, A. Li, B. Guo, X. Yan and G. He, *Small*, 2021, **17**, 2101858.
91 A. R. Spencer, E. Shirzaei Sani, J. R. Soucy, C. C. Corbet, A. Primbetova, R. A. Koppes and N. Annabi, *ACS Appl. Mater. Interfaces*, 2019, **11**, 30518–30533.
92 S. Cao, X. Tong, K. Dai and Q. Xu, *J. Mater. Chem. A*, 2019, **7**, 8204–8209.
93 Y. Xu, M. Cui, P. A. Patsis, M. Guenther, X. Yang, K. Eckert and Y. Zhang, *ACS Appl. Mater. Interfaces*, 2019, **11**, 7715–7724.
94 L. Huang, X. Yang, L. Deng, D. Ying, A. Lu, L. Zhang, A. Yu and B. Duan, *ACS Appl. Mater. Interfaces*, 2021, **13**, 16106–16117.
95 M. Rai, A. Yadav and A. Gade, *Biotechnol. Adv.*, 2009, **27**, 76–83.
96 R. R. Palem, K. Madhusudana Rao and T. J. Kang, *Carbohydr. Polym.*, 2019, **223**, 115074.
97 H. Ji, X. Song, H. Cheng, L. Luo, J. Huang, C. He, J. Yin, W. Zhao, L. Qiu and C. Zhao, *ACS Appl. Mater. Interfaces*, 2020, **12**, 31079–31089.
98 P. Deng, F. Chen, H. Zhang, Y. Chen and J. Zhou, *ACS Appl. Mater. Interfaces*, 2021, **13**, 52333–52345.
99 D. Gan, W. Xing, L. Jiang, J. Fang, C. Zhao, F. Ren, L. Fang, K. Wang and X. Lu, *Nat. Commun.*, 2019, **10**, 1487.
100 Y. Zhao, Z. H. Li, S. L. Song, K. R. Yang, H. Liu, Z. Yang, J. C. Wang, B. Yang and Q. Lin, *Adv. Funct. Mater.*, 2019, **29**, 1901474.
101 Z. Li, Y. Zhao, Z. Wang, M. Ren, X. Wang, H. Liu, Q. Lin and J. Wang, *Adv. Healthcare Mater.*, 2022, **11**, 2102535.
102 C. Wang, X. Jiang, H.-J. Kim, S. Zhang, X. Zhou, Y. Chen, H. Ling, Y. Xue, Z. Chen, M. Qu, L. Ren, J. Zhu, A. Libanori, Y. Zhu, H. Kang, S. Ahadian, M. R. Dokmeci, P. Servati, X. He, Z. Gu, W. Sun and A. Khademhosseini, *Biomaterials*, 2022, **285**, 121479.
103 P. Baei, S. Jalili-Firoozinezhad, S. Rajabi-Zeleti, M. Tafazzoli-Shadpour, H. Baharvand and N. Aghdami, *Mater. Sci. Eng., C*, 2016, **63**, 131–141.
104 A. Navaei, H. Saini, W. Christenson, R. T. Sullivan, R. Ros and M. Nikkhah, *Acta Biomater.*, 2016, **41**, 133–146.
105 Z. Deng, M. Li, Y. Hu, Y. He, B. Tao, Z. Yuan, R. Wang, M. Chen, Z. Luo and K. Cai, *Chem. Eng. J.*, 2021, **420**, 129668.
106 Y. Zhang, W. Fan, K. Wang, H. Wei, R. Zhang and Y. Wu, *J. Photochem. Photobiol., B*, 2019, **192**, 49–54.
107 C. Chai, Y. Guo, Z. Huang, Z. Zhang, S. Yang, W. Li, Y. Zhao and J. Hao, *Langmuir*, 2020, **36**, 10448–10459.
108 J. Cheng, J. Shang, S. Yang, J. Dou, X. Shi and X. Jiang, *Adv. Funct. Mater.*, 2022, **32**, 2200444.
109 C. Xu, Y. Chang, P. Wu, K. Liu, X. Dong, A. Nie, C. Mu, Z. Liu, H. Dai and Z. Luo, *Adv. Funct. Mater.*, 2021, **31**, 2104440.
110 X. Song, X. Wang, J. Zhang, S. Shen, W. Yin, G. Ye, L. Wang, H. Hou and X. Qiu, *Biomaterials*, 2021, **273**, 120811.
111 M. Jia and M. Rolandi, *Adv. Healthcare Mater.*, 2020, **9**, 1901372.

112 X. Ma, C. Wang, W. Yuan, X. Xie and Y. Song, *ACS Appl. Polym. Mater.*, 2021, **3**, 6586–6597.
113 S. Li, L. Wang, W. Zheng, G. Yang and X. Jiang, *Adv. Funct. Mater.*, 2020, **30**, 2002370.
114 H. Guo, M. Bai, Y. Zhu, X. Liu, S. Tian, Y. Long, Y. Ma, C. Wen, Q. Li, J. Yang and L. Zhang, *Adv. Funct. Mater.*, 2021, **31**, 2106406.
115 F. Wang, S. Wang, L. Nan, J. Lu, Z. Zhu, J. Yang, D. Zhang, J. Liu, X. Zhao and D. Wu, *Front. Bioeng. Biotech.*, 2022, **10**, 833887.
116 L. Fan, Z. He, X. Peng, J. Xie, F. Su, D.-X. Wei, Y. Zheng and D. Yao, *ACS Appl. Mater. Interfaces*, 2021, **13**, 53541–53552.
117 D. Li, X. Fei, L. Xu, Y. Wang, J. Tian and Y. Li, *J. Colloid Interface Sci.*, 2022, **627**, 942–955.
118 S. Ding, Z. Lyu, X. Niu, Y. Zhou, D. Liu, M. Falahati, D. Du and Y. Lin, *Biosens. Bioelectron.*, 2020, **149**, 111830.
119 A. M. Curreri, S. Mitragotri and E. E. L. Tanner, *Adv. Sci.*, 2021, **8**, 2004819.
120 S. Khorshidi and A. Karkhaneh, *J. Biomed. Mater. Res., Part A*, 2018, **106**, 718–724.
121 L. Wang, S. Hu, M. W. Ullah, X. Li, Z. Shi and G. Yang, *Carbohydr. Polym.*, 2020, **249**, 116829.
122 M. Zheng, X. Wang, O. Yue, M. Hou, H. Zhang, S. Beyer, A. M. Blocki, Q. Wang, G. Gong, X. Liu and J. Guo, *Biomaterials*, 2021, **276**, 121026.
123 X. Yan, W.-W. Fang, J. Xue, T.-C. Sun, L. Dong, Z. Zha, H. Qian, Y.-H. Song, M. Zhang, X. Gong, Y. Lu and T. He, *ACS Nano*, 2019, **13**, 10074–10084.
124 Y. Liang, M. Wang, Z. Zhang, G. Ren, Y. Liu, S. Wu and J. Shen, *Chem. Eng. J.*, 2019, **378**, 122043.
125 X. Liu, A. L. Miller II, S. Park, B. E. Waletzki, Z. Zhou, A. Terzic and L. Lu, *ACS Appl. Mater. Interfaces*, 2017, **9**, 14677–14690.
126 M. Uz and S. K. Mallapragada, *J. Indian Inst. Sci.*, 2019, **99**, 489–510.
127 L. Zhou, L. Fan, X. Yi, Z. Zhou, C. Liu, R. Fu, C. Dai, Z. Wang, X. Chen, P. Yu, D. Chen, G. Tan, Q. Wang and C. Ning, *Acs Nano*, 2018, **12**, 10957–10967.
128 L.-H. Peng, X.-H. Xu, Y.-F. Huang, X.-L. Zhao, B. Zhao, S.-Y. Cai, M.-J. Xie, M.-Z. Wang, T.-J. Yuan, Y. He, Z. Xu, J.-Q. Gao and C. Gao, *Adv. Funct. Mater.*, 2020, **30**, 2001751.
129 J. Jiao, F. Wang, J.-J. Huang, J.-J. Huang, Z.-A. Li, Y. Kong and Z.-J. Zhang, *Chem. Eng. J.*, 2021, **426**, 131826.
130 V. R. Feig, S. Santhanam, K. W. McConnell, K. Liu, M. Azadian, L. G. Brunel, Z. Huang, H. Tran, P. M. George and Z. Bao, *Adv. Mater. Technol.*, 2021, **6**, 2100162.
131 Y. Hu, Z. Chen, H. Wang, J. Guo, J. Cai, X. Chen, H. Wei, J. Qi, Q. Wang, H. Liu, Y. Zhao and R. Chai, *ACS Nano*, 2022, **16**, 1868–1879.
132 T. Hu, M. Shi, X. Zhao, Y. Liang, L. Bi, Z. Zhang, S. Liu, B. Chen, X. Duan and B. Guo, *Chem. Eng. J.*, 2022, **428**, 131017.
133 Z. Cui, N. C. Ni, J. Wu, G.-Q. Du, S. He, T. M. Yau, R. D. Weisel, H.-W. Sung and R.-K. Li, *Theranostics*, 2018, **8**, 2752–2764.
134 Z. Zhang, X. Zhao, C. Wang, Y. Huang, Y. Han and B. Guo, *Acta Biomater.*, 2022, **151**, 197–209.
135 V. Martinelli, G. Cellot, F. M. Toma, C. S. Long, J. H. Caldwell, L. Zentilin, M. Giacca, A. Turco, M. Prato, L. Ballerini and L. Mestroni, *Nano Lett.*, 2012, **12**, 1831–1838.
136 X. Zhao, B. Guo, H. Wu, Y. Liang and P. X. Ma, *Nat. Commun.*, 2018, **9**, 2784.
137 G. Thakral, J. LaFontaine, B. Najafi, T. K. Talal, P. Kim and L. A. Lavery, *Diabet. Foot Ankle*, 2013, **4**, 22081.
138 M. Ashrafi, T. Alonso-Rasgado, M. Baguneid and A. Bayat, *Exp. Dermatol.*, 2017, **26**, 171–178.
139 H. Lei and D. Fan, *Chem. Eng. J.*, 2021, **421**, 129578.
140 R. Dong, P. X. Ma and B. Guo, *Biomaterials*, 2020, **229**, 119584.
141 M. Talikowska, X. Fu and G. Lisak, *Biosens. Bioelectron.*, 2019, **135**, 50–63.
142 J. Qu, X. Zhao, P. X. Ma and B. L. Guo, *Acta Biomater.*, 2018, **72**, 55–69.
143 Y. Liang, Z. Li, Y. Huang, R. Yu and B. Guo, *Acs Nano*, 2021, **15**, 7078–7093.
144 M.-S. Kim, G.-W. Oh, Y.-M. Jang, S.-C. Ko, W.-S. Park, I.-W. Choi, Y.-M. Kim and W.-K. Jung, *Mater. Sci. Eng., C*, 2020, **107**, 110352.
145 J. Li, F. Yu, G. Chen, J. Liu, X.-L. Li, B. Cheng, X.-M. Mo, C. Chen and J.-F. Pan, *ACS Appl. Mater. Interfaces*, 2020, **12**, 2023–2038.
146 R. Yu, M. Li, Z. Li, G. Pan, Y. Liang and B. Guo, *Adv. Healthcare Mater.*, 2022, **11**, 2102749.
147 C. Wu, L. Shen, Y. Lu, C. Hu, Z. Liang, L. Long, N. Ning, J. Chen, Y. Guo, Z. Yang, X. Hu, J. Zhang and Y. Wang, *ACS Appl. Mater. Interfaces*, 2021, **13**, 52308–52320.
148 X. Jin, Y. Shang, Y. Zou, M. Xiao, H. Huang, S. Zhu, N. Liu, J. Li, W. Wang and P. Zhu, *ACS Appl. Mater. Interfaces*, 2020, **12**, 56681–56691.
149 C. Wang, C. Liang, R. Wang, X. Yao, P. Guo, W. Yuan, Y. Liu, Y. Song, Z. Li and X. Xie, *Biomater. Sci.*, 2020, **8**, 313–324.
150 P. Zhou, Y. Xia, X. Cheng, P. Wang, Y. Xie and S. Xu, *Biomaterials*, 2014, **35**, 10033–10045.
151 R. S. L. Aparna, R. G. S. V. Prasad and N. P. Nirmal, *Sci. Adv. Mater.*, 2016, **8**, 1470–1477.
152 S. W. Sawyer, P. Dong, S. Venn, A. Ramos, D. Quinn, J. A. Horton and P. Soman, *Biomed. Phys. Eng. Express*, 2017, **4**, 015005.
153 S. Qian, Z. Yan, Y. Xu, H. Tan, Y. Chen, Z. Ling and X. Niu, *RSC Adv.*, 2019, **9**, 12001–12009.
154 Y. Liang, Y. Liang, H. Zhang and B. Guo, *Asian J. Pharm. Sci.*, 2022, **17**, 353–384.
155 Y. Zhao, Z. Li, Q. Li, L. Yang, H. Liu, R. Yan, L. Xiao, H. Liu, J. Wang, B. Yang and Q. Lin, *Macromol. Rapid Commun.*, 2020, **41**, 2000441.
156 T. V. Patil, D. K. Patel, S. D. Dutta, K. Ganguly, A. Randhawa and K.-T. Lim, *Appl. Sci.*, 2021, **11**, 9550.
157 Z. Xu, S. Han, Z. Gu and J. Wu, *Adv. Healthcare Mater.*, 2020, **9**, 1901502.
158 M. Kharaziha, A. Baidya and N. Annabi, *Adv. Mater.*, 2021, **33**, 2100176.

159 J. Qu, X. Zhao, Y. Liang, T. Zhang, P. X. Ma and B. Guo, *Biomaterials*, 2018, **183**, 185–199.
160 S. Xing, M. Yan, Y. Yang, Y. Wang, X. Hu, B. Ma and X. Kang, *J. Cluster Sci.*, 2022, 1–12, DOI: **10.1007/s10876-022-02240-7**.
161 K. Zhang, J. Li, J. Jin, J. Dong, L. Li, B. Xue, W. Wang, Q. Jiang and Y. Cao, *Mater. Design*, 2020, **196**, 109092.
162 Z. Jia, J. Gong, Y. Zeng, J. Ran, J. Liu, K. Wang, C. Xie, X. Lu and J. Wang, *Adv. Funct. Mater.*, 2021, **31**, 2010461.
163 S. Saghazadeh, C. Rinoldi, M. Schot, S. S. Kashaf, F. Sharifi, E. Jalilian, K. Nuutila, G. Giatsidis, P. Mostafalu, H. Derakhshandeh, K. Yue, W. Swieszkowski, A. Memic, A. Tamayol and A. Khademhosseini, *Adv. Drug Delivery Rev.*, 2018, **127**, 138–166.
164 S. Municoy, M. I. Álvarez Echazú, P. E. Antezana, J. M. Galdopórpora, C. Olivetti, A. M. Mebert, M. L. Foglia, M. V. Tuttolomondo, G. S. Alvarez, J. G. Hardy and M. F. Desimone, *Int. J. Mol. Sci.*, 2020, **21**, 4724.
165 G. Cirillo, M. Curcio, U. G. Spizzirri, O. Vittorio, P. Tucci, N. Picci, F. Iemma, S. Hampel and F. P. Nicoletta, *Eur. Polym. J.*, 2017, **90**, 1–12.
166 T.-H. Kim, W.-Y. Jeon, Y. Ji, E. J. Park, D. S. Yoon, N.-H. Lee, S.-M. Park, N. Mandakhbayar, J.-H. Lee, H.-H. Lee and H.-W. Kim, *Biomaterials*, 2021, **275**, 120948.
167 X. Zhao, Y. Liang, Y. Huang, J. He, Y. Han and B. Guo, *Adv. Funct. Mater.*, 2020, **30**, 1910748.
168 W. Cao, S. Peng, Y. Yao, J. Xie, S. Li, C. Tu and C. Gao, *Acta Biomater.*, 2022, **152**, 60–73.
169 C. Fan, W. Yang, L. Zhang, H. Cai, Y. Zhuang, Y. Chen, Y. Zhao and J. Dai, *Biomaterials*, 2022, **288**, 121689.
170 F. Chen, M. Wu, Q. Dong, M. Ke, X. Liang, J. Ai, Q. Cheng, L. Cai, Z. Tong and Y. Chen, *Composites, Part B*, 2022, **238**, 109903.
171 H. Huang, X. Zhang, Z. Dong, X. Zhao and B. Guo, *J. Colloid Interface Sci.*, 2022, **625**, 817–830.
172 W. Wang, Z. Li, H. Xu, L. Qiao, X. Zhang, Y. Zhao, Z. Dong, H. Huang, X. Zhao and B. Guo, *Mater. Design*, 2022, **222**, 111041.
173 J. Pang, L. Wang, Y. Xu, M. Wu, M. Wang, Y. Liu, S. Yu and L. Li, *Carbohydr. Polym.*, 2020, **240**, 116360.
174 F. Huang, T. Chen, J. Chang, C. Zhang, F. Liao, L. Wu, W. Wang and Z. Yin, *Int. J. Biol. Macromol.*, 2021, **167**, 434–445.
175 M. Parchehbaf-Kashani, H. Ansari, E. Mahmoudi, M. Barekat, M. Sepantafar, S. Rajabi and S. Pahlavan, *ACS Appl. Bio Mater.*, 2021, **4**, 4849–4861.
176 C. Liu, L. Fan, Z. Tian, H. Wen, L. Zhou, P. Guan, Y. Luo, C. Chan, G. Tan, C. Ning, L. Rong and B. Liu, *Bioact. Mater.*, 2021, **6**, 3892–3903.